LBNL-40100
UC-401
Preprint

ERNEST ORLANDO LAWRENCE BERKELEY NATIONAL LABORATORY

Crossed Molecular Beam Study of the Reaction Br + O_3

Jingsong Zhang, Tzong-Tsong Miau,
and Yuan T. Lee
Chemical Sciences Division

March 1997
Submitted to
Journal of Physical Chemistry

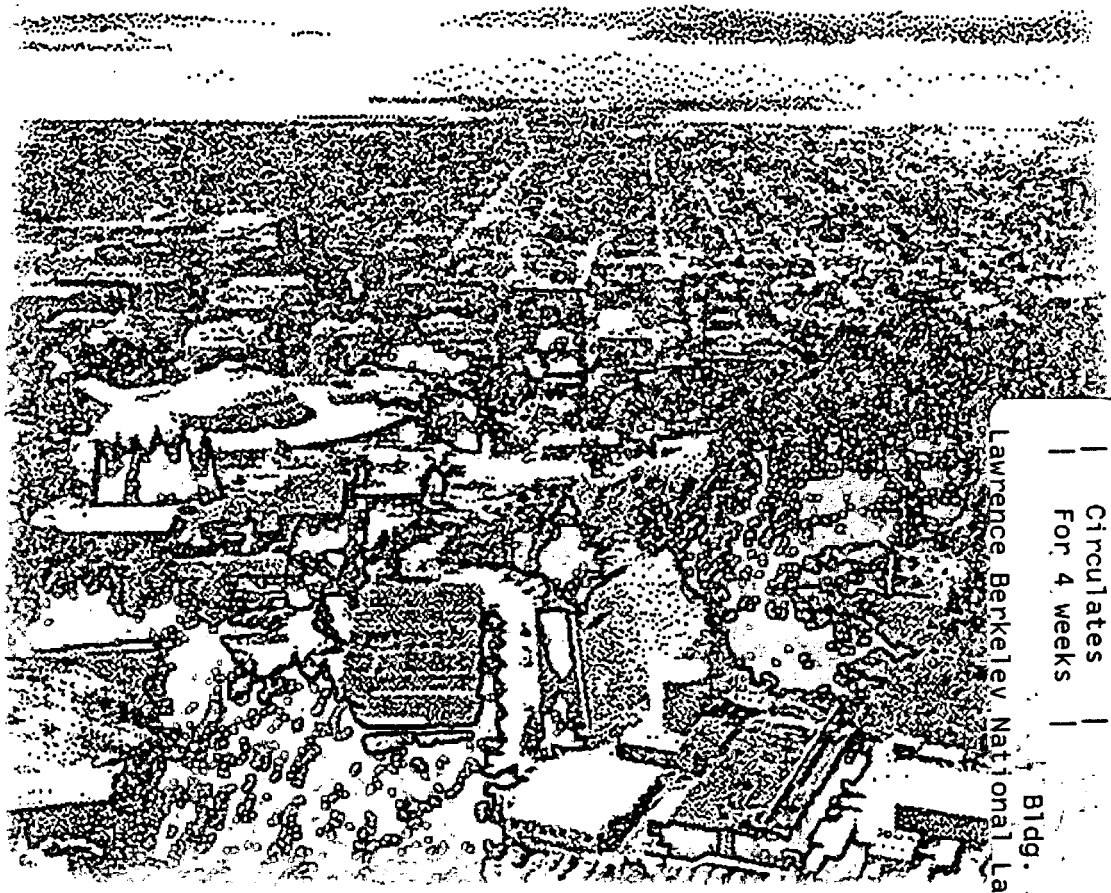

LOAN COPY
Circulates
For 4 weeks
Lawrence Berkeley National Laboratory
Bldg. 50 Library
Copy 2
LBNL-40100

DISCLAIMER

This document was prepared as an account of work sponsored by the United States Government. While this document is believed to contain correct information, neither the United States Government nor any agency thereof, nor The Regents of the University of California, nor any of their employees, makes any warranty, express or implied, or assumes any legal responsibility for the accuracy, completeness, or usefulness of any information, apparatus, product, or process disclosed, or represents that its use would not infringe privately owned rights. Reference herein to any specific commercial product, process, or service by its trade name, trademark, manufacturer, or otherwise, does not necessarily constitute or imply its endorsement, recommendation, or favoring by the United States Government or any agency thereof, or The Regents of the University of California. The views and opinions of authors expressed herein do not necessarily state or reflect those of the United States Government or any agency thereof, or The Regents of the University of California.

Ernest Orlando Lawrence Berkeley National Laboratory
is an equal opportunity employer.

DISCLAIMER

This document was prepared as an account of work sponsored by the United States Government. While this document is believed to contain correct information, neither the United States Government nor any agency thereof, nor the Regents of the University of California, nor any of their employees, makes any warranty, express or implied, or assumes any legal responsibility for the accuracy, completeness, or usefulness of any information, apparatus, product, or process disclosed, or represents that its use would not infringe privately owned rights. Reference herein to any specific commercial product, process, or service by its trade name, trademark, manufacturer, or otherwise, does not necessarily constitute or imply its endorsement, recommendation, or favoring by the United States Government or any agency thereof, or the Regents of the University of California. The views and opinions of authors expressed herein do not necessarily state or reflect those of the United States Government or any agency thereof or the Regents of the University of California.

LBNL-40100
UC-401

Crossed Molecular Beam Study of the Reaction Br + O_3

Jingsong Zhang, Tzong-Tsong Miau, and Yuan T. Lee

Department of Chemistry
University of California, Berkeley

and

Chemical Sciences Division
Ernest Orlando Lawrence Berkeley National Laboratory
University of California
Berkeley, California 94720

March 1997

This work was supported by the Director, Office of Energy Research, Office of Basic Energy Sciences, Chemical Sciences Division, of the U.S. Department of Energy under Contract No. DE-AC03-76SF00098.

Recycled Paper

CROSSED MOLECULAR BEAM STUDY OF THE REACTION Br + O_3

Jingsong Zhang,* Tzong-Tsong Miau, and Yuan T. Lee
Chemical Sciences Division, Lawrence Berkeley National Laboratory,
and
Department of Chemistry, University of California,
Berkeley, California 94720

ABSTRACT

The reaction of ground-state Br($^2P_{3/2}$) atom with ozone molecule has been studied by the crossed molecular beams technique at five different center-of-mass (CM) collision energies ranging from 5 kcal/mole to 26 kcal/mole. Product CM translational energy distribution and angular distribution have been derived from experimental data. The average product translational energy ranges from 30%-60% of the total available energy. BrO product is forward and sideways scattered with respect to the Br atom in the CM frame. With the increase of collision energy, the fraction of the total energy channeled into products' translation is increased, and the BrO product is scattered to a more forward direction. The product translational energy release depends strongly on the CM scattering angles, with the translational energy in the forward direction larger than that in the backward direction. The Br + O_3 reaction is a direct reaction, and the Br atom most likely attacks a terminal oxygen atom of the ozone molecule. Detailed comparison of the experimental results for the Cl + O_3 and Br + O_3 reactions shows that these two reactions have very similar mechanisms. Ozone electronic structure seems to play a central role in determining the reaction mechanisms.

* Present address: Department of Chemistry, University of California, Riverside, CA 92521-0403.
Fax: 909-787-4713; E-mail: jszhang@ucrac1.ucr.edu

I. INTRODUCTION

The reaction $Br + O_3 \rightarrow BrO + O_2$ is important in stratospheric chemistry along with the reaction $Cl + O_3 \rightarrow ClO + O_2$.[1] They play the key roles in catalytic ozone destruction cycles. The ClO dimer and ClO/BrO mechanisms in which these two reactions are involved are responsible for most of the Antarctic stratosphere ozone loss.[2-6] The reaction $Br + O_3$ is one of the initial steps in the ClO/BrO cycle of ozone destruction.

A large number of kinetic studies on ozone reactions with radicals such as $Cl + O_3$ and $Br + O_3$ have been carried out.[7-13] Pre-exponential factors of these reactions were found to be very similar and insensitive to the reaction exothermicity;[10,12,13] the rate coefficients for these reactions correlated with electron affinities of the radical atoms instead of the reaction exothermicity.[10] It was suggested that the transition-state structures of these reactions were insensitive to the radical and these reactions proceeded via early transition states that best resembled the reactant ozone.[10,11,12] Based on the information from the kinetic studies, the reaction $Br + O_3$ is expected to be very similar to the reaction $Cl + O_3$.

Vibrational excitation of the BrO product from the $Br + O_3$ reaction was observed in a flash photolysis study of Br_2-O_3 system by McGrath and Norrish.[14] Their flash photolysis light was filtered by a soda glass filter so that only the Br_2 molecule, and not the O_3 molecule in the Br_2-O_3 mixture, could be dissociated. BrO absorption was observed after a time delay of several μs. v" = 0 progression of BrO absorption was predominant, but BrO absorption bands with v" up to 4 were also visible in the experiments. Similar to the $Cl + O_3$ reaction, the BrO product had considerable vibrational excitation.

There has been almost no theoretical study on the $Br + O_3$ reaction. However, due to the similarity of the $Br + O_3$ and the $Cl + O_3$ reactions, the semi-empirical study of the $Cl + O_3$ reaction by Farantos and Murrell[15] may provide some insight into the reaction mechanism. An early transition state was located on the semi-empirical ClO_3 potential energy surface (PES).[15] Classic trajectory calculations carried out on this PES at thermal collision energy showed that the ClO product was predominantly forward scattered with respect to the Cl atom in the CM system and there was no long-lived complex formation. The calculations also showed that at thermal collision energy 49% of the total available energy went into translation of the products and there

was a large amount of vibrational energy in ClO. Michael and Payne[9] used the activated complex theory to calculate the pre-exponential factor of the Br + O_3 reaction. They assumed a collinear approach and used the BEBO method to determine an intermediate configuration that was quite close to the reactants. More information was needed to accurately estimate the bending frequencies, therefore, the comparison between the calculated and the experimental pre-exponential factors was not conclusive.

We have previously reported a crossed molecular beam study of the Cl + O_3 reaction.[16] A large product translational energy release and sideways and forward ClO scattering with respect to the Cl atom were observed. It was concluded that the Cl + O_3 reaction proceeded as a direct reaction and the Cl atom most likely abstracted a terminal O atom of the ozone molecule. In this work, we extend the crossed molecular beam study to the Br + O_3 reaction, which was carried out at five collision energies. With the detailed experimental information such as the product CM angular and translational energy distributions, we would like to compare with the Cl + O_3 reaction and further probe the mechanisms of the reactions of atomic radicals and ozone molecule.

II. EXPERIMENTAL

The experimental setup in this study is similar to that in the Cl + O_3 study.[16] The universal crossed molecular beam apparatus has been described in detail previously.[17,18] Supersonic bromine atom and ozone molecule beams were crossed at 90° in a scattering chamber under a vacuum of ~ 10^{-7} Torr. The scattered products were detected by a differentially-pumped mass spectrometric detector which rotated in the plane of the two beams. The typical electron energy of the electron impact ionizer was 180 eV, and the ion energy was 90 eV. The size of the collision zone was 3 × 3 × 3 mm^3, and under normal conditions the whole collision zone was viewed by the detector.

Bromine atom beam was produced by thermal dissociation of Br_2 in rare gas mixtures in a resistively heated high-density graphite nozzle source.[19] The Br_2/rare gas mixtures were generated by passing He, Ar or Kr through liquid bromine (Fisher or Mallinkcrodt, reagent grade, without any further purification) in a glass bubbler held at an ice/water bath (total pressure 700

Torr, Br_2 vapor pressure ~ 60 Torr at 0 °C). For the highest collision energy used in this experiment, helium gas was passed through the Br_2 bubbler held at -9 °C (Br_2 vapor pressure 40 Torr, total pressure 700 Torr) in a low-temperature bath. The high-temperature graphite source had a nozzle of 0.12 mm diameter and was heated to ~ 1700 °C. A very large fraction of Br_2 (≥ 97%) was thermally dissociated, as confirmed by a mass spectrometric measurement. Ozone beam has been described in detail previously.[16] 7% ozone/rare gas mixtures with 300 Torr total pressure was expanded through a 0.12 mm diameter nozzle. The nozzle tip was heated to ~ 80 °C to minimize ozone dimers.

Velocity distributions of the Br and O_3 beams were measured by time-of-flight (TOF) technique. The beam parameters were obtained from fitting the experimental TOF spectra by using a program KELVIN,[20,21] which convoluted over the known apparatus functions. Typical beam parameters in this experiment are given in Table 1. Collision energy was varied by seeding Br_2 and O_3 in different rare gases and by changing Br_2 concentration in the gas mixtures. Most-probable collision energies E_{coll} and the spread of collision energies are listed in Table 2.

Product TOF spectra from the reactive scattering were measured by using the cross-correlation method with a time resolution of 5μs/channel.[22] The nominal flight path was 30.1 cm. BrO product was monitored. The mass spectrometer was set at m/e = 95 with low resolution to detect $Br^{79}O$ isotope species, while a small amount of $Br^{81}O$ was collected as well. Total counting times ranged from 0.5 to 6 hours per laboratory angle.

BrO product laboratory angular distributions, except for the experiment at E_{coll} = 18.5 kcal/mole, were measured by modulating the ozone beam with a 150 Hz tuning folk chopper. Signals with ozone beam on and off were recorded and the difference gave the net reactive signal. Total counting time per angle ranged from 3 to 10 minutes. For E_{coll} = 18.5 kcal/mole, BrO angular distribution was obtained by integrating the TOF spectra at various laboratory angles.

The main scattering chamber was lined with a liquid-nitrogen cooled cold panel along the walls and an additional cryogenically cooled copper panel was placed against the differential wall and facing the detector. These arrangements were effective in reducing the BrO background for both TOF and angular measurements.

III. RESULTS AND ANALYSIS

Laboratory angular and TOF distributions were recorded at five CM collision energies from 5 kcal/mole to 26 kcal/mole. Experimental conditions for four collision energies are listed in Table 2. Newton diagrams of these four collision energies are shown in Figs. 2, 7, 12, and 17. The circles stand for the maximum CM recoil velocity of the BrO product if all the available energy channels into products' translation. Angular and TOF distributions were recorded at m/e = 95, corresponding to $Br^{79}O^+$.

Laboratory angular distribution and TOF spectra were fitted by using a forward-convolution method. The FORTRAN program is an improved version based on a previous program.[23] The goal of the analysis is to find the product angular and translational energy distributions in the CM frame. It starts with a trial form for the CM product flux-energy distribution. The program transforms this trial CM flux distribution into the laboratory flux distribution; it then generates the laboratory angular distribution and TOF spectra, after convoluting over the measured beam velocity distributions and the known apparatus functions such as the spread of collision angles, the detector acceptance angles, and the length of the ionizer. The program scales the calculated spectra to the experimental data and makes the comparison. This procedure is repeated so as to optimize the CM flux distribution iteratively until a best fit for the experimental data is found.

Initially we tried to fit the experimental data by using an energy-angle separable form for the CM flux distribution. In this trial form, the CM flux distribution was expressed as a product of $T(\theta)$, the CM product angular distribution, and $P(E_T)$, the CM product relative translational energy distribution. As in the $Cl + O_3$ study, a separable form of the CM flux distribution was inadequate. Using a single set of $T(\theta)$ and $P(E_T)$ functions that could well describe the TOF spectra at large laboratory angles ($\Theta > 40°$), the fittings for the TOF spectra at small laboratory angles ($\Theta < 25°$) were clearly too slow compared with the experimental data. In the CM frame, a faster forward contribution in the CM flux distribution was needed to make a satisfactory fit to our experimental data which had very good signal-to-noise ratio. It seemed that the CM product translational energy release coupled with the CM angles and it was larger in the forward direction than in the backward direction. This behavior is exactly the same as in the $Cl + O_3$

reaction.

To account for the coupling effect in a simplified way, a combination of different sets of uncoupled $T(\theta)$ and $P(E_T)$ was used. CM product flux distribution was expressed as the weighted sum of the products of different sets of $T(\theta)$ and $P(E_T)$:[16]

$$I_{CM}(\theta, E_T) = \sum_{i=1}^{n} w_i \cdot T_i(\theta) \cdot P_i(E_T) \qquad (1)$$

Each $P_i(E_T)$ was normalized so that $\int P_i(E_T)dE_T = 1$. The total CM angular distribution could therefore be expressed as:

$$I_{CM}(\theta) = \int_0^{\infty} I_{CM}(\theta, E_T)dE_T = \sum_{i=1}^{n} w_i \cdot T_i(\theta) \qquad (2)$$

Quite satisfactory fits to the experimental data can be achieved by using a trial $I_{CM}(\theta, E_T)$ function combined from two different sets of $T(\theta)$ and $P(E_T)$. $T(\theta)$ was chosen in a point form, and $P(E_T)$ was chosen in a RRK-type functional form.[16] Experimental and calculated laboratory angular distributions at four collision energies are shown in Figs. 2, 7, 12, and 17. Experimental and fitted laboratory TOF spectra are in Figs. 3, 8, 13, and 18. Average translational energy releases versus CM angles and total CM angular distributions are in Figs. 4, 9, 14, and 19. The relative translational energy distributions at various CM angles are plotted in Figs. 5, 10, 15, and 20. Using the optimized CM flux-energy distribution $I_{CM}(\theta, E_T)$, the CM flux distributions in velocity space $I_{CM}(\theta, u)$ [$I_{CM}(\theta, u) \propto u \cdot I_{CM}(\theta, E_T)$] both in contour maps and in 3-dimensional surface curves are plotted in Figs. 6, 11, 16, and 21.

Results for the Br + O_3 reaction are very similar to those from the Cl + O_3 reaction. Laboratory angular distributions are quite broad, partially due to the large product translational energy release. The large intensity at negative laboratory angles (Θ = -20° to -10°) is not due to any impurity in the Br beam, since no m/e = 95 signal was observed as O_3 was substituted by CO_2, and our data fittings gave quite reasonable reproduction of this intensity for the four different collision energies and kinematics. In the CM frame, the angular distributions are also

quite broad, with large intensities for the sideways and forward scattering. The CM angular distributions do not have a forward-backward symmetry. Peak of the angular distribution shifts from 90° to 60° and finally 30° with the collision energy increased, and the peak becomes more predominant. Experimental data at E_{coll} = 26 kcal/mole, which is under the most favorable kinematics, allows us to obtain a quite confident fit for the CM angular distribution down to CM angle 10°. The intensity decrease from 30° to 10° in the CM frame at E_{coll} = 26 kcal/mole is quite obvious. At lower collision energies, the CM angular distribution within 20° is less certain; however, the trend of decrease in this region is still clear.

Product translational energy release is large, which is especially evident in the TOF spectra at the laboratory angles near the CM angle Θ_{CM} for collision energy E_{coll} = 26 kcal/mole and 18.5 kcal/mole. A fast and a slow peak in these TOF spectra indicate that the CM recoil velocity of the BrO product is very large. All translational energy release probabilities $P(E_T)$ peak quite far away from 0 kcal/mole; they are smooth and almost symmetric. Product translational energy is higher at small CM angles than at wide angles. With the collision energy increased, the fraction of the total energy channeled into translation and the width of the translational energy distribution increase; furthermore, the angular dependence of the translational energy release increases as well, i.e., the difference between the fast and slow translational energy releases becomes larger. These trends of the translational energy release are shown in Figs. 5, 10, 15, 20, 22, and 23, as well as in Tables 3 and 4.

We tried to detect the reaction channel $Br + O_3 \rightarrow BrO_2 + O$ (Fig. 1). There are two types of BrO_2 isomers: asymmetric BrOO and symmetric OBrO. OBrO could be observed by the mass spectrometer,[24] but the threshold of OBrO + O channel is not clear due to insufficient thermodynamic data. BrOO molecule is less stable than OBrO (Br and O_2 are bonded by only ~ 1 kcal/mole),[7,24-26] and it may not survive in the electron bombardment ionizer. The reaction channel BrOO + O would be open above about 22 kcal/mole collision energy; above ~ 23 kcal/mole collision energy, BrOO might undergo decomposition. We detected no signal at m/e = 111 at 26 kcal/mole collision energy. As in the $Cl + O_3$ reaction, the reaction channel $Br + O_3 \rightarrow BrO_2 + O$ appears to be a very minor channel.

IV. DISCUSSION

The CM product angular and translational energy distributions of the Br + O_3 reaction are very similar to those in the Cl + O_3 reaction, indicating that both reactions proceed through similar mechanisms. The reaction Br + O_3 is also a direct reaction, as the CM angular distribution has the predominant forward-sideways peak and does not have the typical forward-backward symmetry of a reaction via a persistent long-lived complex.[27] The strong couplings between the product translational energy and the CM angles, as well as the repulsive translational energy release, also indicates a direct reaction mechanism.

Besides the similar CM angular and translational energy distributions in the Br + O_3 and Cl + O_3 reactions,[16] the collision energy dependence of these distributions and the couplings between the translational energy distributions and the CM scattering angles are also very similar. Essentially, dynamic information for both reactions obtained from the crossed molecular beam studies shows that these two reactions are very much alike.[16] This similarity supports the suggestion from the early kinetic studies that the transition-state structures of these reactions were mostly determined by the configuration of ozone molecule.[10-12] The similarity also qualitatively agrees with the theoretical calculations which indicated that the configuration of the reaction intermediate was like that of the ozone molecule,[9,15] and is consistent with the argument by Schaefer and co-workers that ozone electronic structure plays an important role in the reaction mechanism.[28] O_3 molecule can be characterized as a diradical with the two unpaired π electrons in the terminal O atoms.[29] Its center O atom has a closed outer shell of 8 electrons, while the terminal O atom has only 7 outer electrons with a half-filled $2p\pi$ orbital perpendicular to the molecular plane. The two terminal atomic $O2p\pi$ orbitals form the pair of the π molecular orbitals $1a_2$ and $2b_1$; the $1a_2$ orbital (HOMO) is fully occupied by two terminal $O2p\pi$ electrons.

As argued previously,[16] it is unlikely for the Br atom to abstract the central O atom, because of the high repulsion of the lone-pair electrons on the central O atom. This is confirmed by the predominant forward-sideways instead of backward scattering of the BrO product. It is also unlikely for the Br atom to insert into the O-O bond. Similar transition-state configurations of these two reactions imply that the Cl or Br atom probably does not insert to the O-O bond to make the transition-state structure quite different from that of the ozone molecule.

Similar to the Cl + O_3 reaction, the Br atom should abstract the terminal O atom. When the Br atom attacks the π orbital on the O_3 molecule perpendicularly from above the O_3 molecular plane, the interaction has a net overlap between the frontier molecular orbitals and is symmetry-allowed.[30] This collision pathway has a large impact parameter and the BrO product should be scattered in the forward direction. With the increasing collision energy, the forward scattering would become stronger. However, this channel is not able to produce the significant amount of large-angle scattering, especially at high collision energies. The Br atom could attack a terminal O atom in the ozone molecule plane, leading to the sideways and wide-angle scattering. In this coplanar approach, the Br atom has a large range of attacking angles; for a direct reaction, they correspond to a wide range of CM angles into which the product BrO could be scattered.

Similar to the Cl + O_3 reaction, two reaction mechanisms are possible in the Br + O_3 reaction. The rate of increase of the product translational energy with the collision energy varies with CM angles (Figs. 22 and 23). Specifically, the product translational energy increases faster for small CM angles than for wide CM angles; the internal energy remains essentially constant for very small scattering angels (Fig. 23). These two different types of collision energy dependences suggest two possible reaction mechanisms. At E_{coll} = 5 kcal/mole the forward scattering channel with large translational energy release seems to be nearly not open, and the forward scattering channel appears to have a higher effective reaction barrier than the wide-angle scattering channel. In a large impact parameter collision such as the out-of-plane approach, a fair amount of translational energy is tied up to rotation of the reaction intermediate and is not effective in overcoming the reaction barrier of the entrance channel, especially when the translational energy is low. Only at high collision energies, the forward scattering with large impact parameter in the out-of-plane approach starts to become important. Of course, the analysis for the out-of-plane collision is also applicable for the large impact parameter collision in the in-plane approach; however, in the coplanar approach, the impact parameter dependence should be smooth, so the large change in CM angle dependence of the translational energy release may not come from the in-plane pathway only.

In summary, the Br atom predominantly attacks the terminal O atom of the ozone molecule. At low collision energy (E_{coll} = 5 kcal/mole), the BrO product is mainly sideways scattered and the product translational energy is ~ 30-40% of the total available energy. The

coplanar collision channel seems to contribute dominantly at low collision energy. At high collision energies (E_{coll} = 14.5 to 26 kcal/mole), the BrO product is forward and sideways scattered and the product translational energy is about 40-65% of the total energy. The in-plane pathway gives significant amount of sideways and forward scattering, while an out-of-plane collision pathway may contribute to the forward scattering as well. Note that the forward scattering at high collision energies is more predominant than that in the Cl + O_3 reaction, possibly due to the heavier mass of the Br atom. The similarity of the experimental results for both Br + O_3 and Cl + O_3[16] is consistent with an early transition state that resembles the reactant ozone molecule, as suggested by the semi-empirical studies[15] and previous kinetic studies.[10,11,12] The internal energy of the products, though not resolved in this experiment, should be largely the vibrational and rotational energy of BrO product for a reaction via early transition state. The predominant forward and sideways scattering and the fall-off in the very small CM angle region, even at the highest collision energy, suggest a quite strong repulsion on the exit channel. An impulsive energy release model predicts 33% of the reaction exoergicity going into the products' translation at the reaction threshold. The extrapolation of the measured product translation energy release to the threshold gives a value of ~ 31%, in good agreement with the impulsive model. Of course, a high-level quantum mechanical calculation on the Br + O_3 reaction is very valuable and can provide more quantitative comparison with the results of this crossed molecular beam study.

Product channels $BrO(^2\Pi) + O_2(^3\Sigma_g^-)$ and $BrO(^2\Pi) + O_2(^1\Delta_g)$ are energetically possible at all collision energies. When E_{coll} is above 6.4 kcal/mole, the third product channel $BrO(^2\Pi) + O_2(^1\Sigma_g^+)$ is also open (Fig. 1). For radical and ozone reactions such as Cl + O_3,[16,31,32] $O(^3P) + O_3$,[33] $H(^2S) + O_3$,[33] and $NO(^2\Pi) + O_3$,[33,34] early experiments have shown none or very little formation of the electronically excited $O_2(^1\Delta_g)$ and $O_2(^1\Sigma_g^+)$ products. In these reactions, when the radical attacks a terminal O atom and the O-O bond between this terminal O atom and the central O atom cleaves, the remaining O-O part of the ozone molecule would undergo minimum change in energy and electronic structure to form the O_2 molecule. The most likely state of the O_2 molecule would be the ground state $O_2(^3\Sigma_g^-)$ because the old π orbitals on this O-O part remain unchanged. The translational energy release probabilities in the Br + O_3 reaction are quite smooth and extend near the maximum available energy, in consistency with a dominant ground-state $O_2(^3\Sigma_g^-)$ channel.

Two bromine spin-orbit states $Br(^2P_{3/2})$ and $Br(^2P_{1/2})$ are separated by 10.5 kcal/mole. Assuming a thermal equilibrium, only ~ 3% of the Br atoms are produced in the spin-orbit excited state $Br(^2P_{1/2})$ in our thermal dissociation source at ~ 2000 K temperature. If $Br(^2P_{1/2})$ is highly reactive, there should be ~ 10.5 kcal/mole more energy release, but no extra energy release was found in the translational energy distributions. The ground-state $Br(^2P_{3/2})$ atom should contribute predominantly in our crossed molecular beam experiment.

V. CONCLUSIONS

We have studied the Br + O_3 reaction by using the crossed molecular beam method at five collision energies from 5 kcal/mole to 26 kcal/mole. CM product angular distribution and translational energy distribution have been derived from experimental data. The product translational energy release is large, with the average ranging from 30%-60% of the total energy. The BrO product is sideways and forward scattered in the CM frame. With the increase of the collision energy, the fraction of the total energy channelled into translation is increased, and the BrO product is scattered into more forward direction with respect to the Br atom. There is a strong coupling between the translational energy release and the CM angles, with the translational energy release in the forward direction larger than that in the backward direction.

It is concluded that the Br + O_3 reaction has a direct reaction mechanism. The Br atom would most likely attack the terminal oxygen atom. The exit channel on the BrO_3 potential energy surface should have a strong repulsion. A high-level quantum mechanical calculation on the Br + O_3 reaction is valuable to compare with the results of the crossed molecular beam study.

The detailed comparison of the results for the Cl + O_3 and the Br + O_3 reactions manifests that these two reactions have the similar mechanism. In the ozone reactions with atomic radicals, ozone electronic structure plays the central role to determine the reaction mechanisms. It is expected that ozone reactions with other atomic radicals such as F + O_3 and I + O_3 should proceed with the similar reaction mechanisms.

ACKNOWLEDGMENT

We thank A. G. Suits and H. F. Davis for helping set up the ozone beam source. This work was supported by the Director, Office of Energy Research, Office of Basic Energy Sciences, Chemical Sciences Division of the U. S. Department of Energy under Contract No. DE-AC03-76SF00098.

REFERENCES

1. R. P. Wayne, Chemistry of Atmospheres (Clarendon Press, Oxford, 1991).
2. L. T. Molina and M. J. Molina, J. Phys. Chem. **91**, 433 (1987).
3. M. B. McElroy, R. J. Salawitch, S. C. Wofsy, and J. A. Logan, Nature **321**, 759 (1986).
4. J. G. Anderson, D. W. Toohey, and W. H. Brune, Science **251**, 39 (1991).
5. J. W. Barrett, P. M. Solomon, R. L. de Zafra, M. Jaramillo, L. Emmons, and A. Parrish, Nature **336**, 455 (1988).
6. S. Solomon, Nature **347**, 347 (1990).
7. M. A. A. Clyne and H. W. Cruse, Trans. Faraday Soc. **66**, 2214 (1970).
8. M. -T. Leu and W. B. DeMore, Chem. Phys. Lett. **48**, 317 (1977).
9. J. V. Michael and W. A. Payne, Int. J. Chem. Kinet. **11**, 799 (1979).
10. D. W. Toohey, W. H. Brune, and J. G. Anderson, Int. J. Chem. Kinet. **20**, 131 (1988) and the references therein.
11. J. M. Nicovich, K. D. Kreutter, and P. H. Wine, Int. J. Chem. Kinet. **22**, 399 (1990) and the references therein.
12. R. Patrick and D. M. Golden, J. Phys. Chem. **88**, 491 (1984).
13. a) D. L. Baulch, R. A. Cox, R. F. Hampson Jr., J. A. Kerr, J. Troe, and R. T. Watson, J. Phys. Chem. Ref. Data. **9**, 295 (1980); b) D. L. Baulch, R. A. Cox, P. J. Crutzen, R. F. Hampson Jr., J. A. Kerr, J. Troe, and R. T. Watson, J. Phys. Chem. Ref. Data. **11**, 327 (1982).
14. a) W. P. McGrath and R. G. W. Norrish, Z. Phys. Chem. **15**, 245 (1958); b) W. P.

McGrath and R. G. W. Norrish, Proc. Roy. Soc. A **254**, 317 (1960).

15. S. C. Farantos and J. N. Murrell, Int. J. Quan. Chem. **14**, 659 (1978).
16. J. Zhang and Y. T. Lee (submitted to J. Phys. Chem.).
17. Y. T. Lee, J. D. McDonald, P. R. LeBreton, and D. R. Herschbach, Rev. Sci. Instrum. **40**, 1402 (1969).
18. R. K. Sparks, Ph. D. Thesis, University of California, Berkeley (1979).
19. J. J. Valentini, M. J. Coggiola, and Y. T. Lee, Rev. Sci. Instrum. **48**, 58 (1977).
20. M. F. Vernon, Ph. D. Thesis, University of California, Berkeley (1983).
21. D. J. Krajnovich, Ph. D. Thesis, University of California, Berkeley (1983).
22. a) K. Sköld, Nucl. Inst. Methods **63**, 114 (1968); b) V. L. Hirshy and J. P. Aldridge, Rev. Sci. Instrum. **42**, 381 (1971); c) G. Comsa, R. David, and B. J. Schumacher, Rev. Sci. Instrum. **52**, 789 (1981).
23. R. J. Buss, Ph. D. Thesis, University of California, Berkeley (1979).
24. N. I. Butkovskaya, I. I. Morozov, V. L. Tal'rose, and E. S. Vasiliev, Chem. Phys. **79**, 21 (1983).
25. J. A. Blake, R. J. Browne, and G. Burns, J. Chem. Phys. **53**, 3320 (1970).
26. S. P. Sander and R. T. Watson, J. Phys. Chem. **85**, 4000 (1981).
27. a) W. B. Miller, S. A. Safron, and D. R. Herschbach, Discuss. Faraday Soc. **44**, 108 (1967); b) W. B. Miller, Ph. D. Thesis, Harvard University (1969).
28. a) M. M. L. Chen, R. W. Wetmore, and H. F. Schaefer III, J. Chem. Phys. **74**, 2938 (1981); b) M. Dupuis, G. Fitzgerald, B. Hammond, W. A. Lester, and H. F. Schaefer III, J. Chem. Phys. **84**, 2691 (1986).
29. P. J. Hay and T. H. Dunning, Jr., J. Chem. Phys. **67**, 2290 (1977).
30. K. Fukui, Reactivity and Structure Concepts in Organic Chemistry, Vol. 2: Theory of Orientation and Stereoselection (Springer-Verlag, New York, 1975).
31. J. W. Vanderzanden and J. W. Birks, Chem. Phys. Lett. **88**, 109 (1982).
32. K. Y. Choo and M. Leu, J. Phys. Chem. **89**, 4832 (1985).
33. N. Washida, H. Akimoto, and M. Okuda, Bull. Chem. Soc. Jpn. **53**, 3496 (1980).
34. M. Gauthier and D. R. Snelling, Chem. Phys. Lett. **20**, 178 (1973).

TABLES

TABLE I. Experimental Beam Parameters.

Beam Condition	Peak Velocity (v_{pk}) (m/s)	Speed Ratio ($v/\Delta v$)
Br (6% Br_2 in He)	2370	5.7
Br (9% Br_2 in He)	1900	5.8
Br (9% Br_2 in Kr)	1020	7.7
O_3 (7% in He)	1280	13.6
O_3 (7% in Ar)	640	12.6

TABLE II. Experimental Conditions.

Br v_{pk} (m/s)	O_3 v_{pk} (m/s)	Collision Energy E_{coll} (kcal/mole)	$\Delta E_{coll}/E_{coll}$	$\Delta E_{coll}/E_{avl}$
2370	1280	26	27%	12%
1900	1280	18.5	23%	9%
1900	640	14.5	31%	10%
1020	640	5	19%	3%

TABLE III. Average Translational Energy Release.

E_{coll}	E_{avl} [a]	$\langle E_T \rangle / E_{avl}$ [b]			$(\Delta \langle E_T \rangle)_{max}$ [c]
		CM angle 10°	CM angel 40°	CM angle 120°	
26	57	0.62	0.56	0.43	11
18.5	49.5	0.58	0.52	0.41	9
14.5	45.5	0.54	0.49	0.37	8
5	36	0.39	0.37	0.33	2

a. Total available energy in kcal/mole.

b. Fraction of average product translational energy at various CM angles.

c. Maximum difference of average translational energy release at small and large CM angles in kcal/mole.

TABLE IV. Peak Translational Energy Release.

E_{coll}	E_{avl}	E_T^{peak}/E_{avl} [a]			$(\Delta E_T^{peak})_{max}$ [b]
		CM angle 10°	CM angel 40°	CM angle 120°	
26	57	0.64	0.57	0.41	13
18.5	49.5	0.59	0.53	0.38	10
14.5	45.5	0.54	0.48	0.35	9
5	36	0.35	0.33	0.30	2

a. Fraction of peak product translational energy at various CM angles.

b. Maximum difference of peak translational energy release at small and large CM angles in kcal/mole.

FIGURE CAPTIONS

Figure 1 Energy level diagram of the Br + O_3 reaction. Thermodynamic values are derived from Refs. 13b, 25, and 26. The solid lines stand for collision energies in the experiment.

Figure 2 Upper: Laboratory angular distribution of the reaction Br + O_3 at E_{coll} = 26 kcal/mole. The filled circles are the experimental data. Error bars stand for 95% confidence limits. The solid lines are the calculated fitting curves.

Lower: Newton diagram for the reaction Br + O_3 at E_{coll} = 26 kcal/mole. The circle stands for the maximum CM velocity of the BrO product. The Br beam is defined as $\Theta = 0°$ in the laboratory frame, and the ozone beam is $\Theta = 90°$.

Figure 3 Laboratory TOF spectra of the BrO product at E_{coll} = 26 kcal/mole. The circles are the experimental data points. The solid lines are the fitting. (a) TOF spectra in the laboratory angles from -15° to 22.5°. (b) TOF spectra in the laboratory angles from 25° to 55°.

Figure 4 Upper: Average translational energy $\langle E_T \rangle$ at different CM angles for E_{coll} = 26 kcal/mole.

Lower: Total CM angular distribution $I_{CM}(\theta)$ at E_{coll} = 26 kcal/mole. The maximum of the relative angular distribution is scaled to unit.

Figure 5 Product translational energy distribution at various CM angles for E_{coll} = 26 kcal/mole. Maximum probabilities are scaled to unit. The maximum translational energy in these plots is the total available energy for the reaction at the most probable collision energy E_{coll} = 26 kcal/mole.

Figure 6 The contour map and the 3-D plot for the CM flux-velocity distribution $I_{CM}(\theta, u)$ at E_{coll} = 26 kcal/mole.

Figure 7 Same as Fig. 2 but at E_{coll} = 18.5 kcal/mole.

Figure 8 Same as Fig. 3 but at E_{coll} = 18.5 kcal/mole. (a) TOF spectra in the laboratory angles from -15° to 27.5°. (b) TOF spectra in the laboratory angles from 30° to 65°.

Figure 9 Same as Fig. 4 but at E_{coll} = 18.5 kcal/mole.

Figure 10 Same as Fig. 5 but at E_{coll} = 18.5 kcal/mole.

Figure 11 Same as Fig. 6 but at E_{coll} = 18.5 kcal/mole.

Figure 12 Same as Fig. 2 but at E_{coll} = 14.5 kcal/mole.

Figure 13 Same as Fig. 3 but at E_{coll} = 14.5 kcal/mole: TOF spectra in the laboratory angles from -15° to 45°.

Figure 14 Same as Fig. 4 but at E_{coll} = 14.5 kcal/mole.

Figure 15 Same as Fig. 5 but at E_{coll} = 14.5 kcal/mole.

Figure 16 Same as Fig. 6 but at E_{coll} = 14.5 kcal/mole.

Figure 17 Same as Fig. 2 but at E_{coll} = 5 kcal/mole.

Figure 18 Same as Fig. 3 but at E_{coll} = 5 kcal/mole: TOF spectra in the laboratory angles from 25° to 55°.

Figure 19 Same as Fig. 4 but at E_{coll} = 5 kcal/mole.

Figure 20 Same as Fig. 5 but at E_{coll} = 5 kcal/mole.

Figure 21 The contour plot of the CM flux distribution $I_{CM}(\theta, u)$ at E_{coll} = 5 kcal/mole for the region where the TOF spectra are measured.

Figure 22 Upper: Fraction of average translational energy in the total energy at different CM angles versus collision energies.

Lower: Fraction of peak translational energy release at different CM angles versus collision energies.

Figure 23 Upper: Average translational energy at different CM angles versus collision energies.

Lower: Average internal energy at different CM angles versus collision energies.

Energy Level Diagram

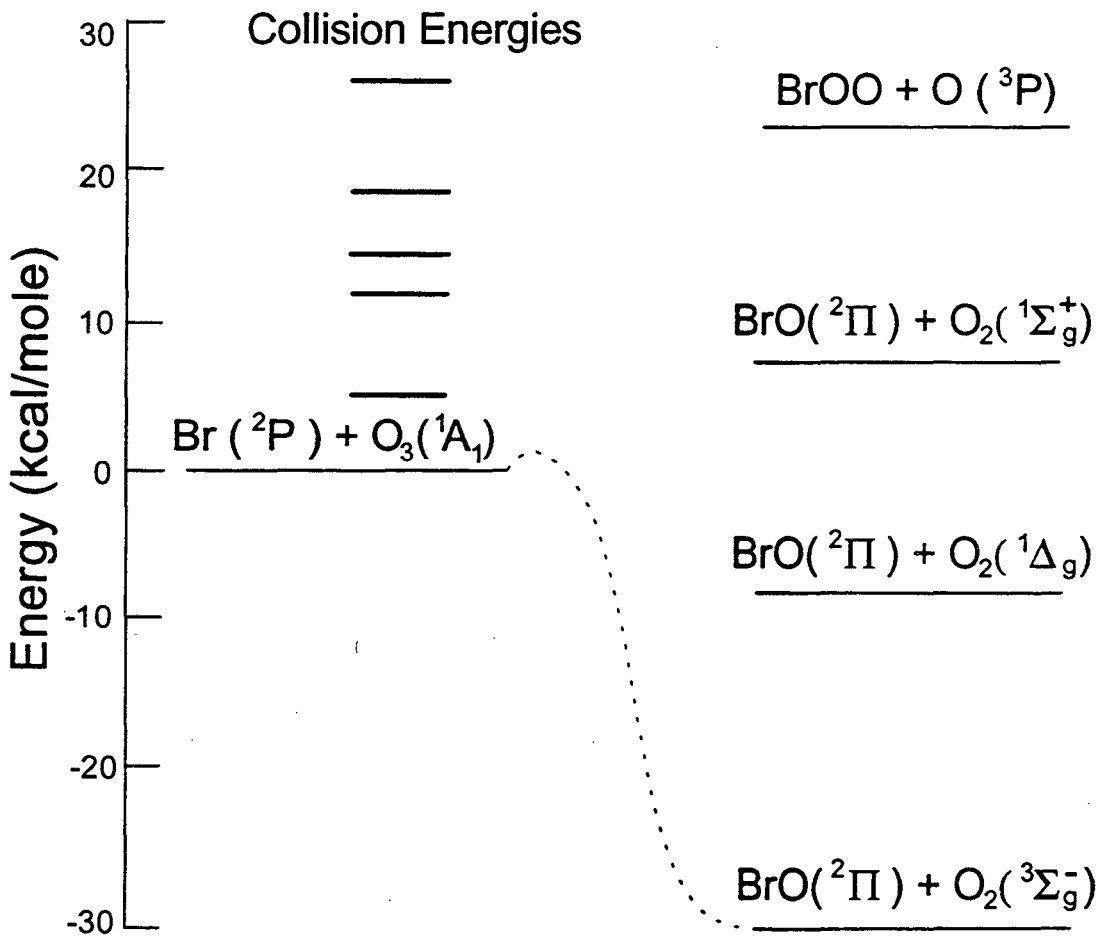

Fig. 1

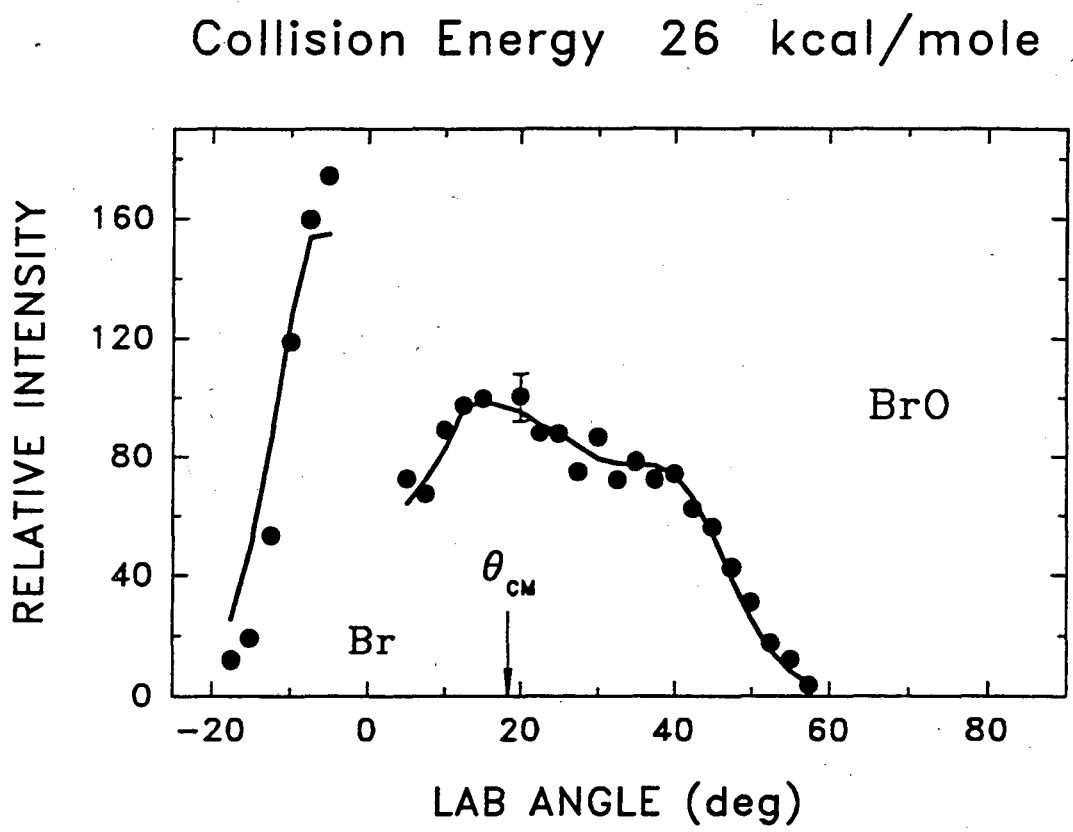
Collision Energy 26 kcal/mole
RELATIVE INTENSITY
160
120
80
40
0
-20
0
20
40
60
80
LAB ANGLE (deg)
BrO
Br
θ_{CM}

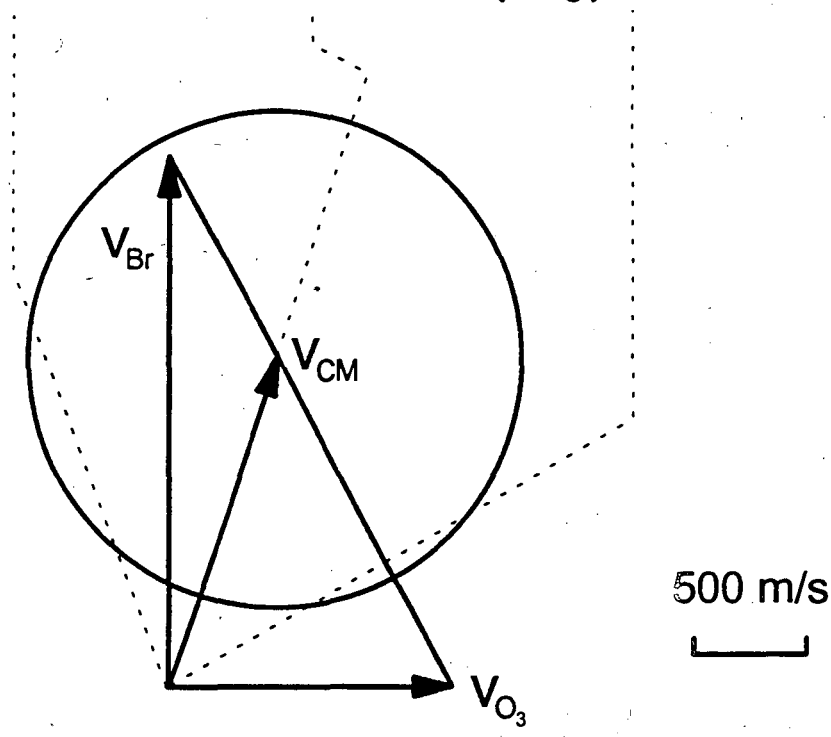
V_{Br}
V_{CM}
V_{O_3}
500 m/s

Fig.

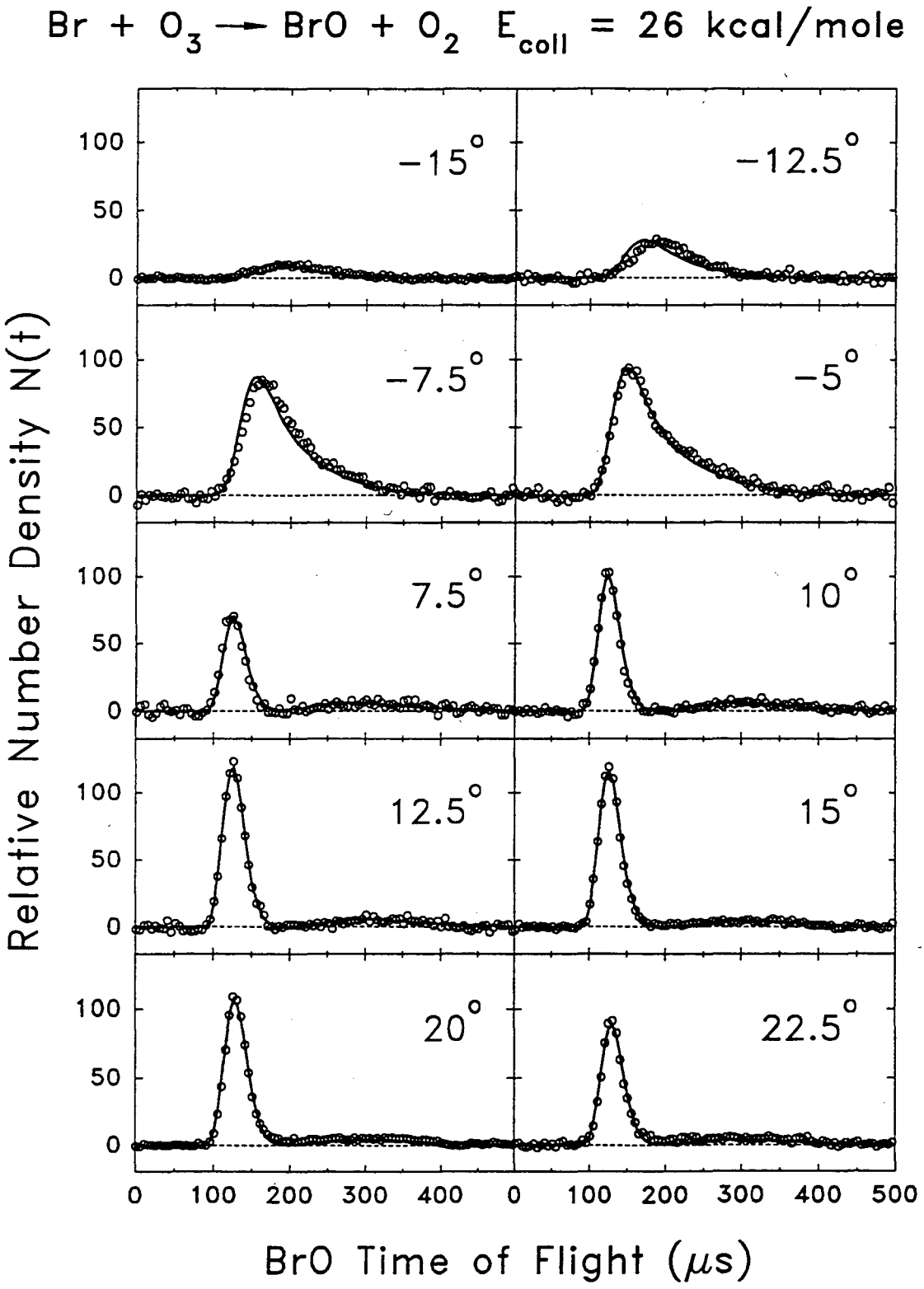
Br + O3 → BrO + O2 Ecoll = 26 kcal/mole
Relative Number Density N(t)
BrO Time of Flight (μs)
−15°
−12.5°
−7.5°
−5°
7.5°
10°
12.5°
15°
20°
22.5°
0
50
100
0
100
200
300
400
500

Fig. 3a

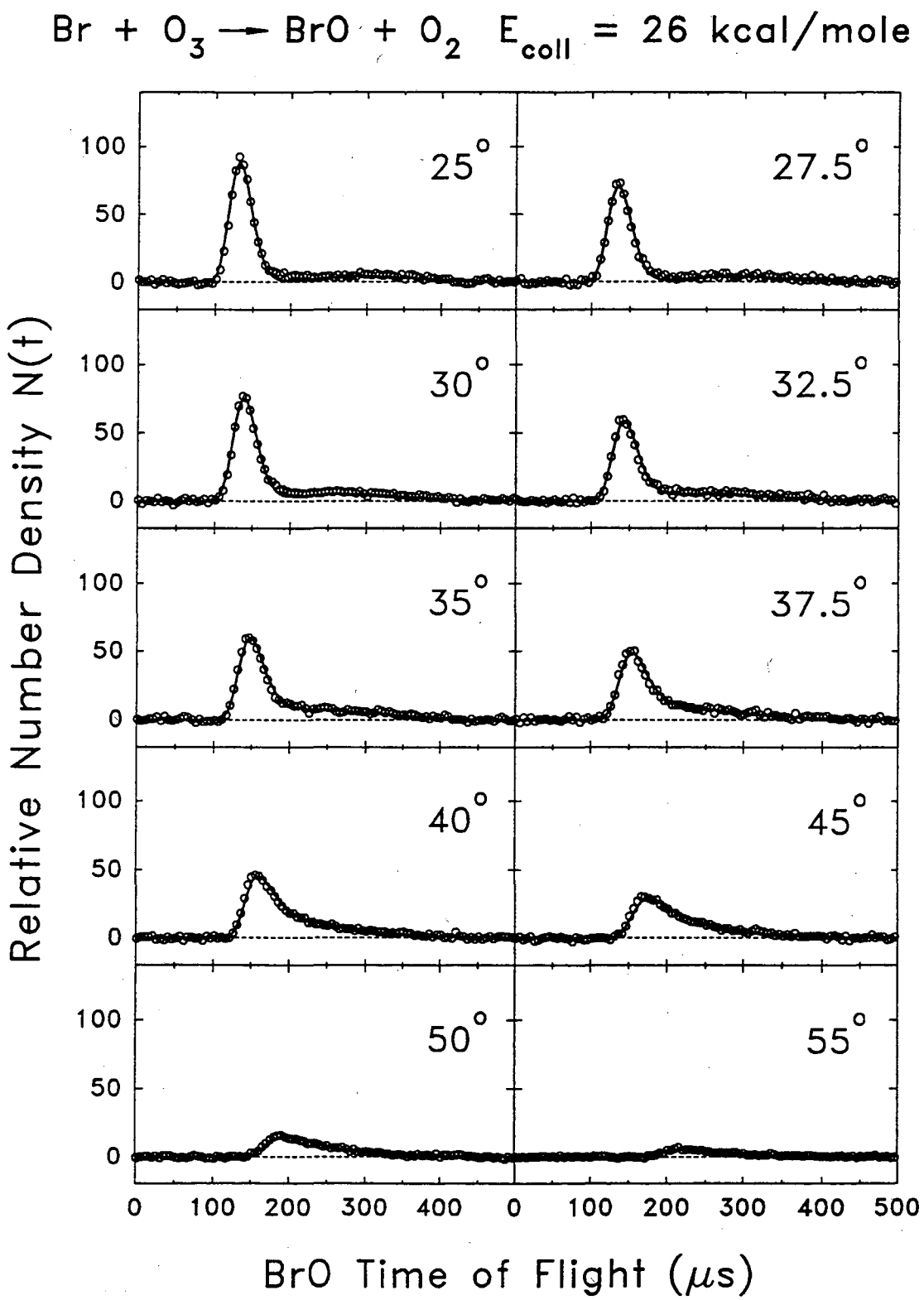
Br + O3 → BrO + O2 Ecoll = 26 kcal/mole
25°
27.5°
30°
32.5°
35°
37.5°
40°
45°
50°
55°
Relative Number Density N(t)
BrO Time of Flight (μs)
0
50
100
0
100
200
300
400
500

3b

Fig.

Collision Energy 26 kcal/mole

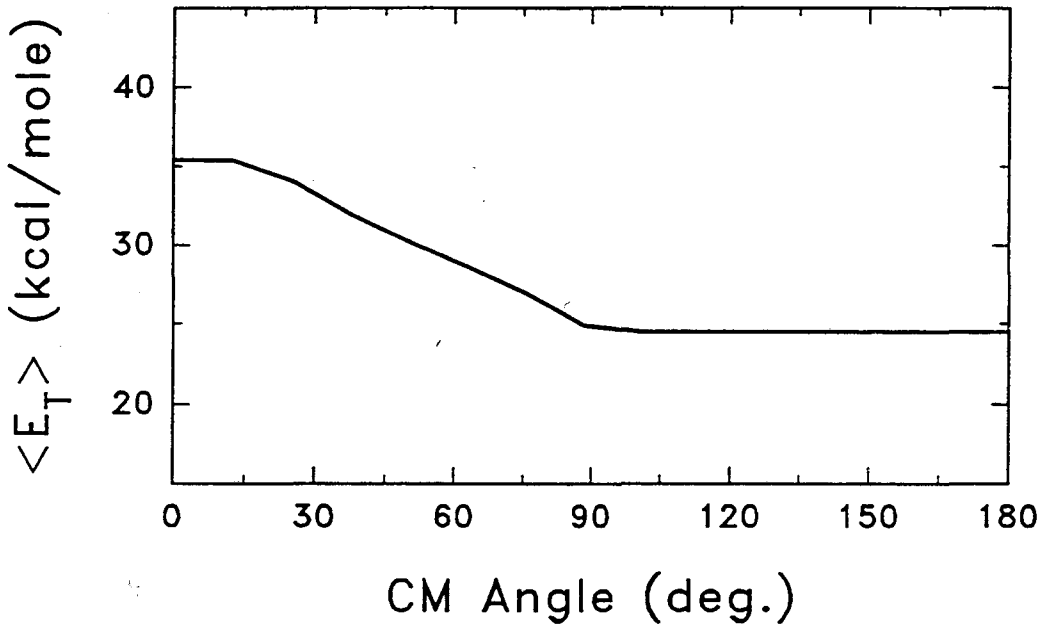

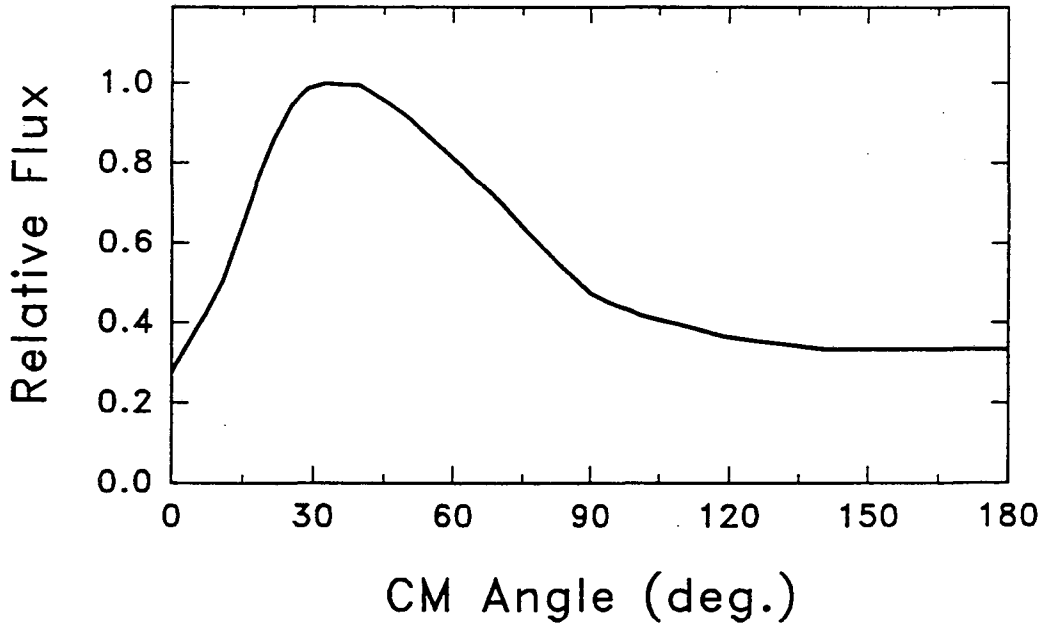

4

Fig. 4

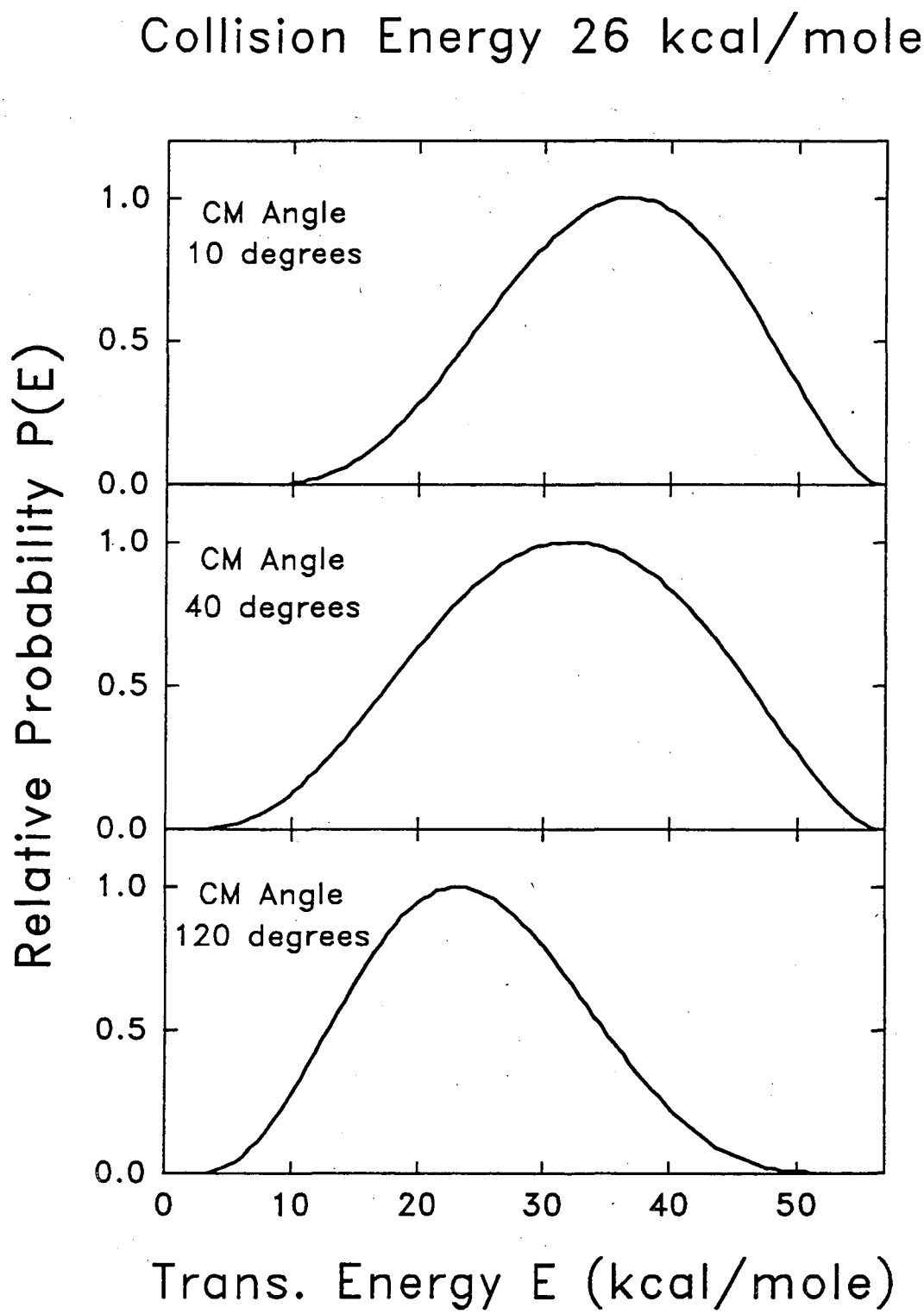
Collision Energy 26 kcal/mole
CM Angle
10 degrees
CM Angle
40 degrees
CM Angle
120 degrees
1.0
0.5
0.0
Relative Probability P(E)
0
10
20
30
40
50
Trans. Energy E (kcal/mole)

5

Fig.

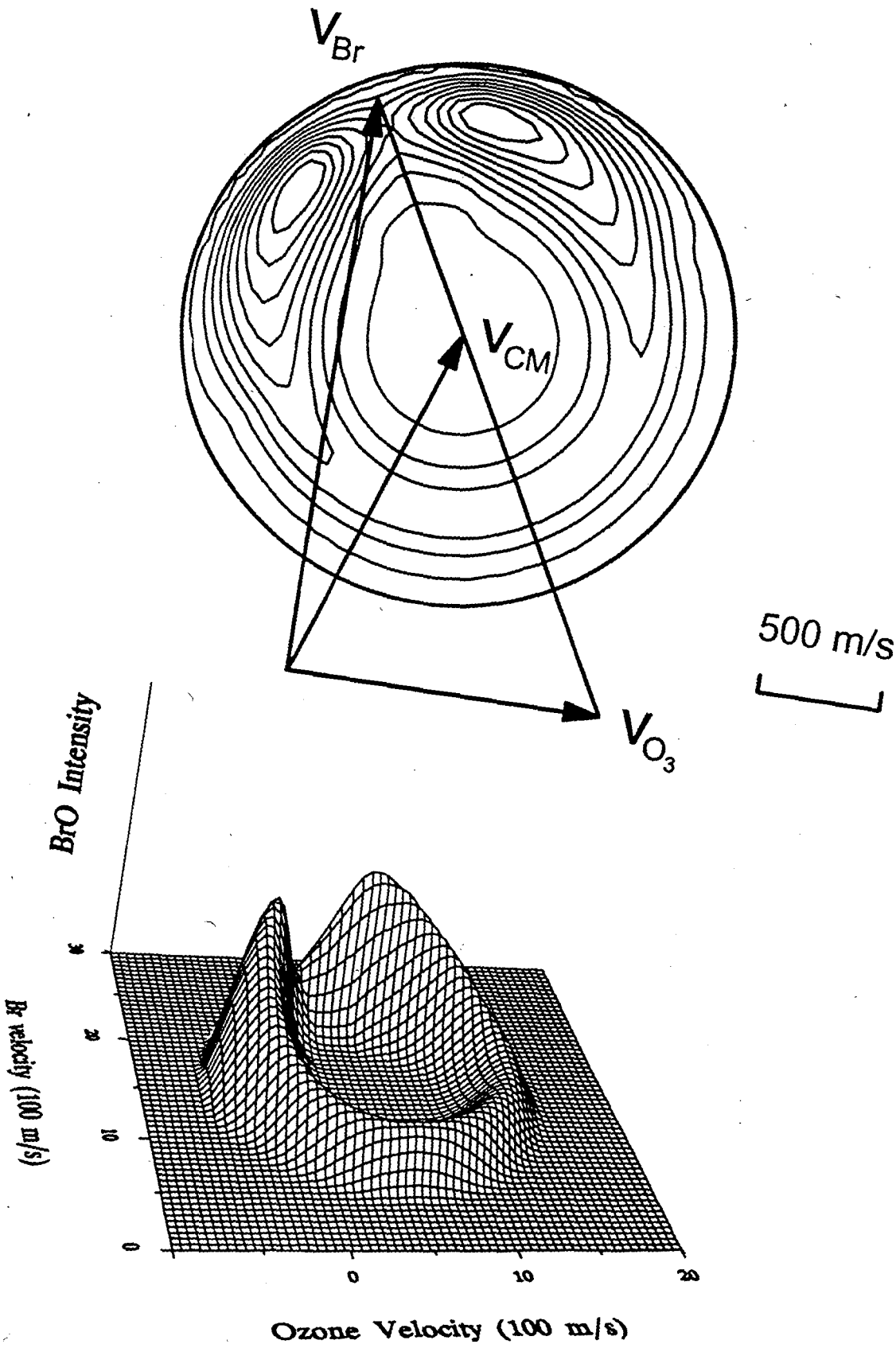
V_{Br}
V_{CM}
V_{O_3}
500 m/s
BrO Intensity
Br velocity (100 m/s)
0
10
20
30
0
10
20
Ozone Velocity (100 m/s)

6

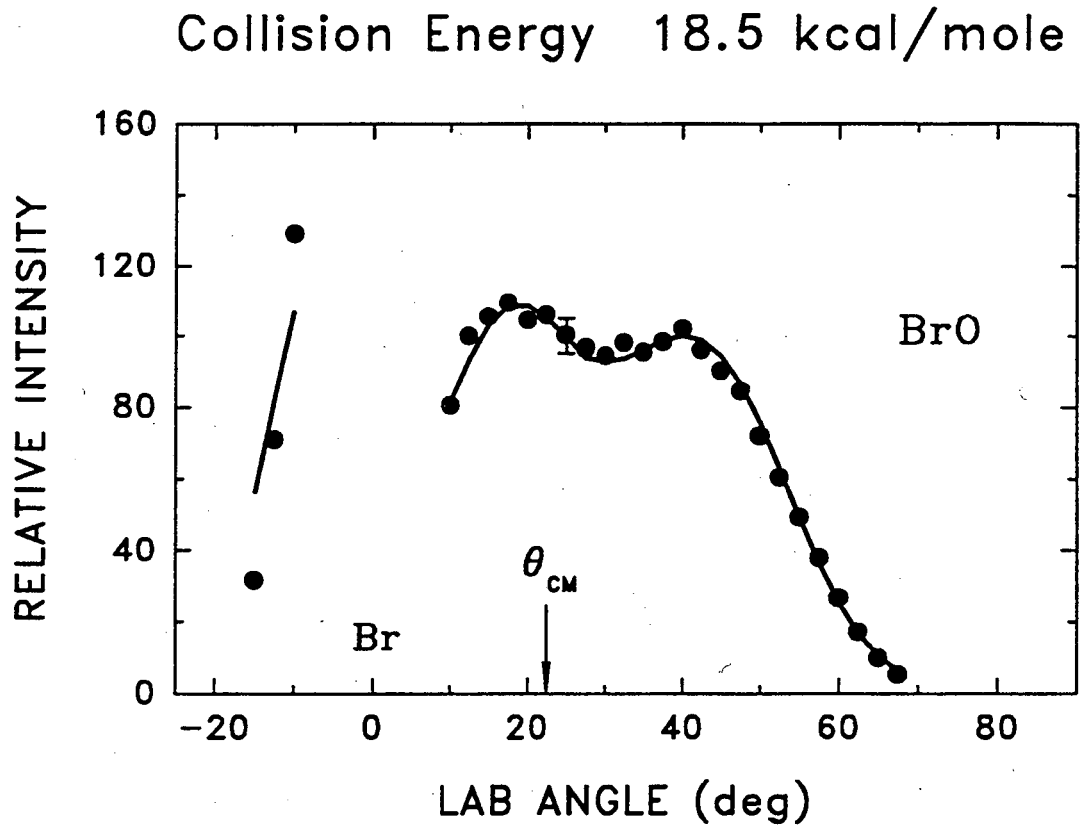
Collision Energy 18.5 kcal/mole
RELATIVE INTENSITY
160
120
80
40
0
-20
0
20
40
60
80
LAB ANGLE (deg)
BrO
Br
θ_{CM}

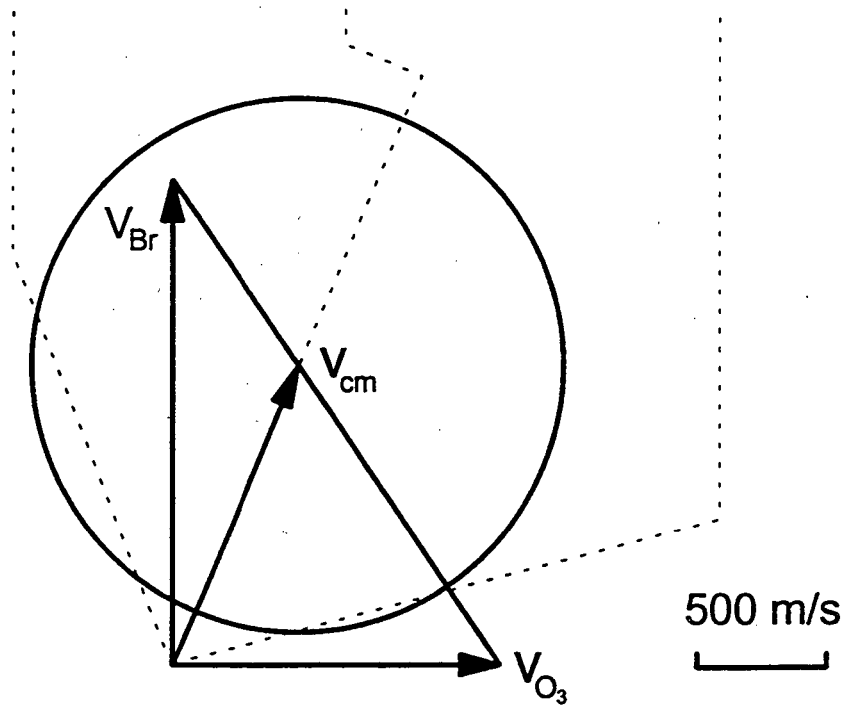
V_{Br}
V_{cm}
V_{O_3}
500 m/s

Fi

$Br + O_3 \rightarrow BrO + O_2 \quad E_{coll} = 18.5$ kcal/mole

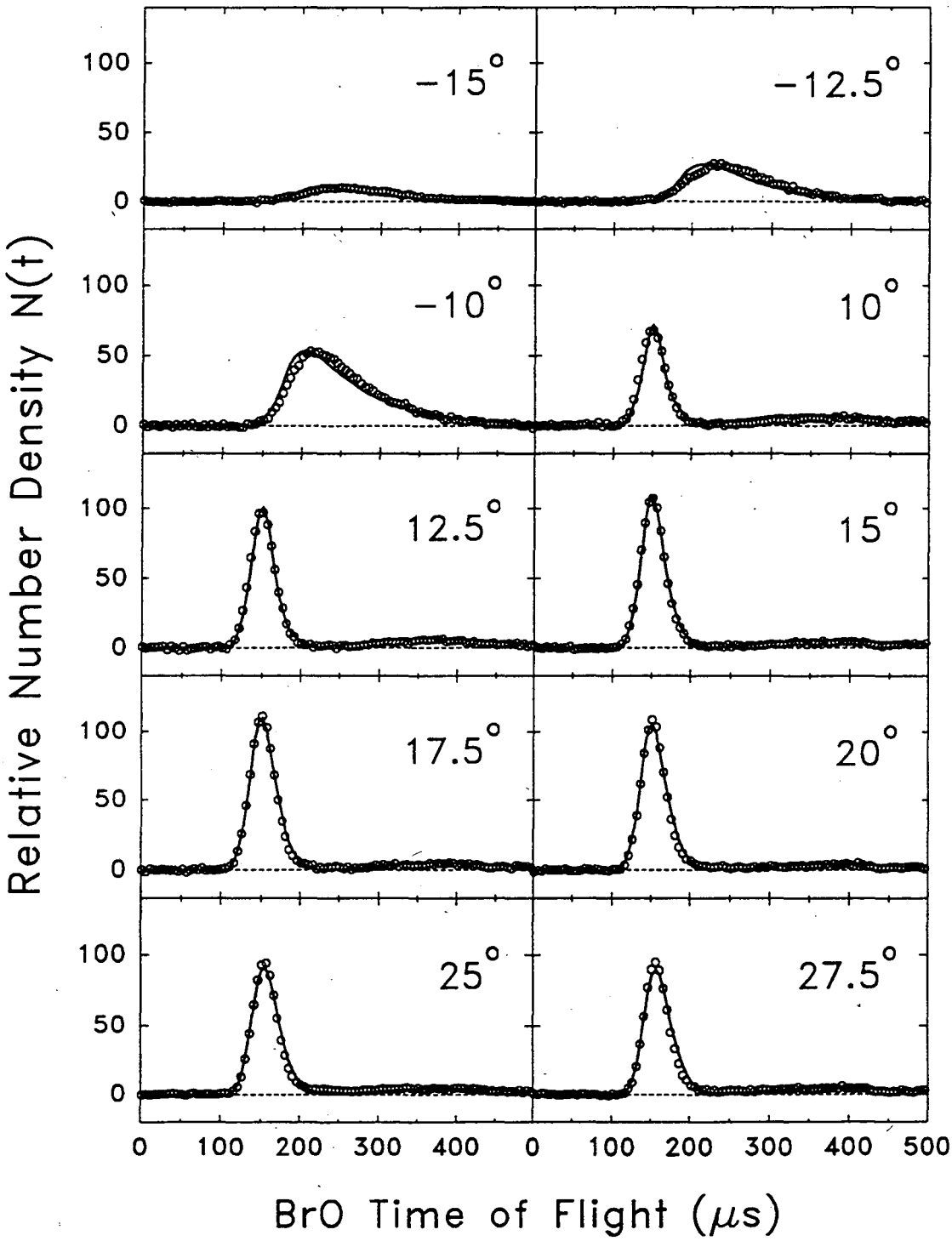

8a

Fig. 8

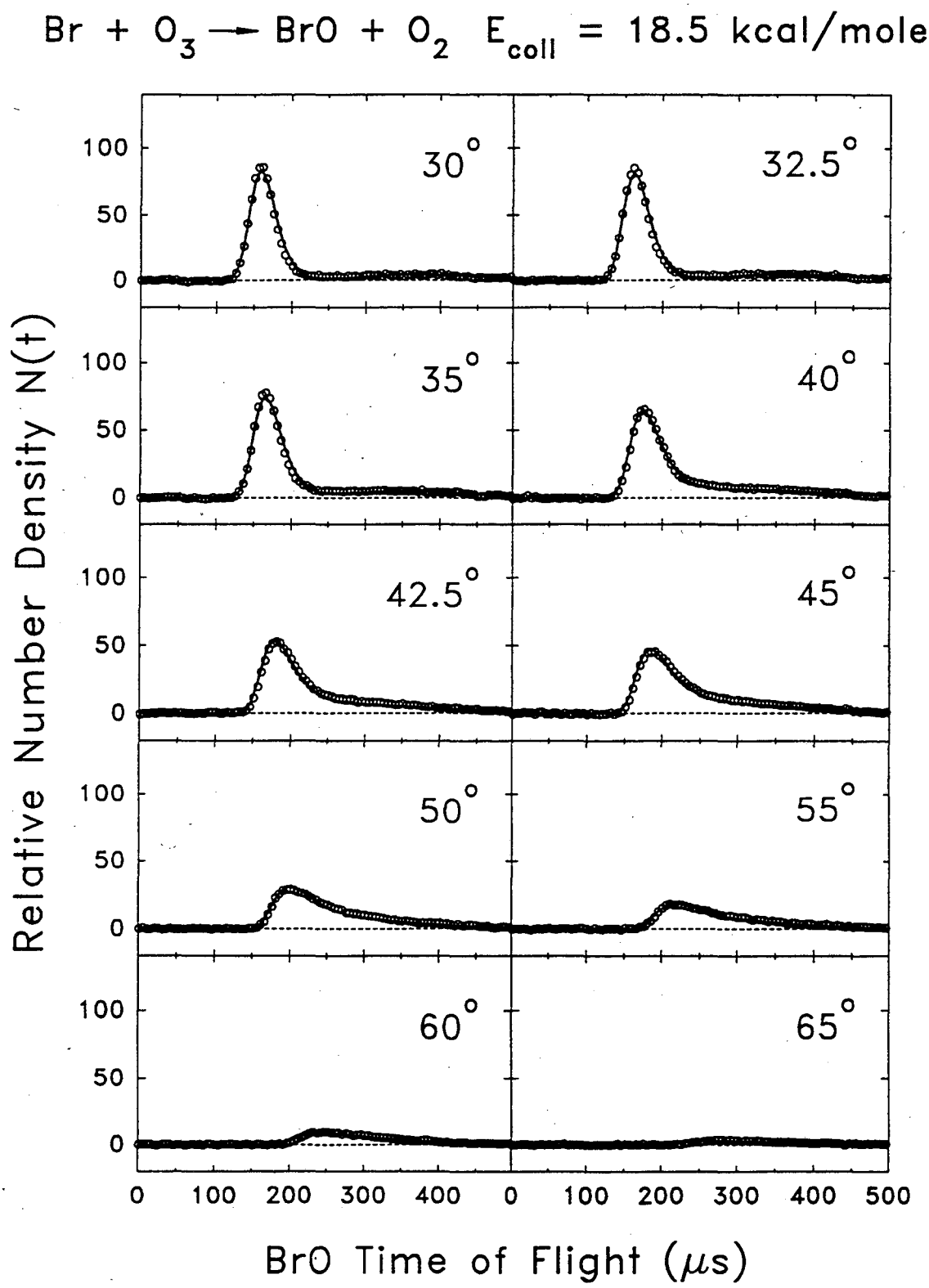
Br + O3 → BrO + O2 Ecoll = 18.5 kcal/mole
30°
32.5°
35°
40°
42.5°
45°
50°
55°
60°
65°
Relative Number Density N(t)
BrO Time of Flight (μs)
0
50
100
0
100
200
300
400
500

Fig. 8b

Collision Energy 18.5 kcal/mole

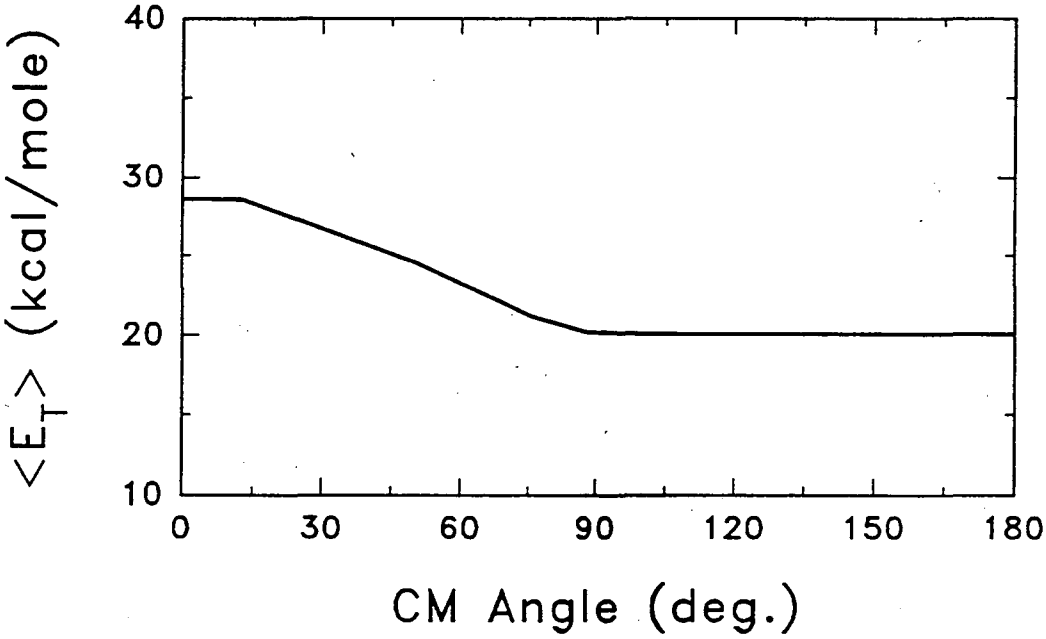

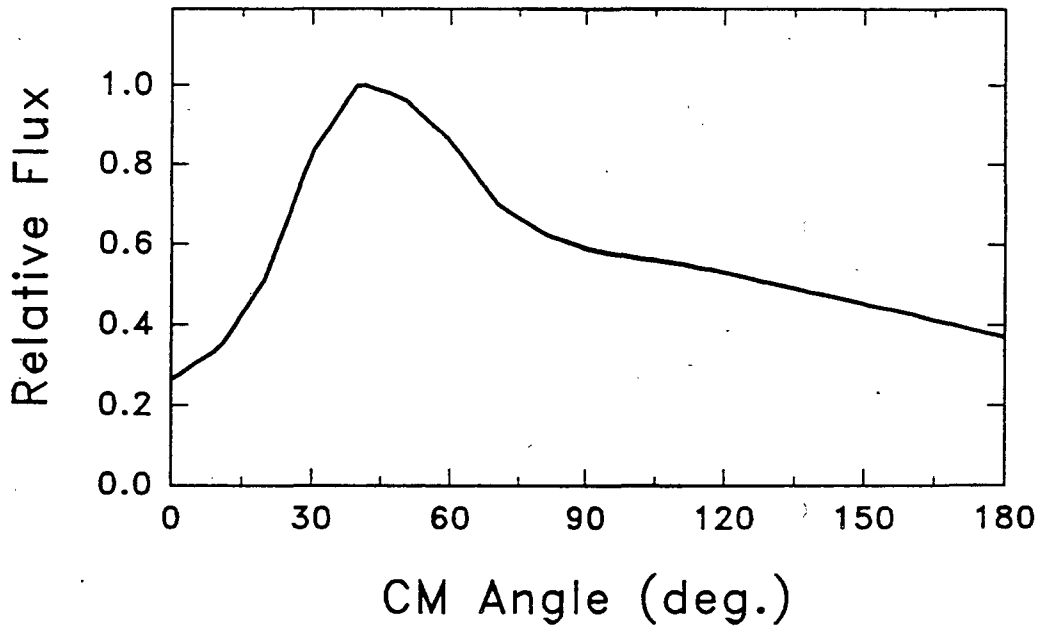

9

Fig.

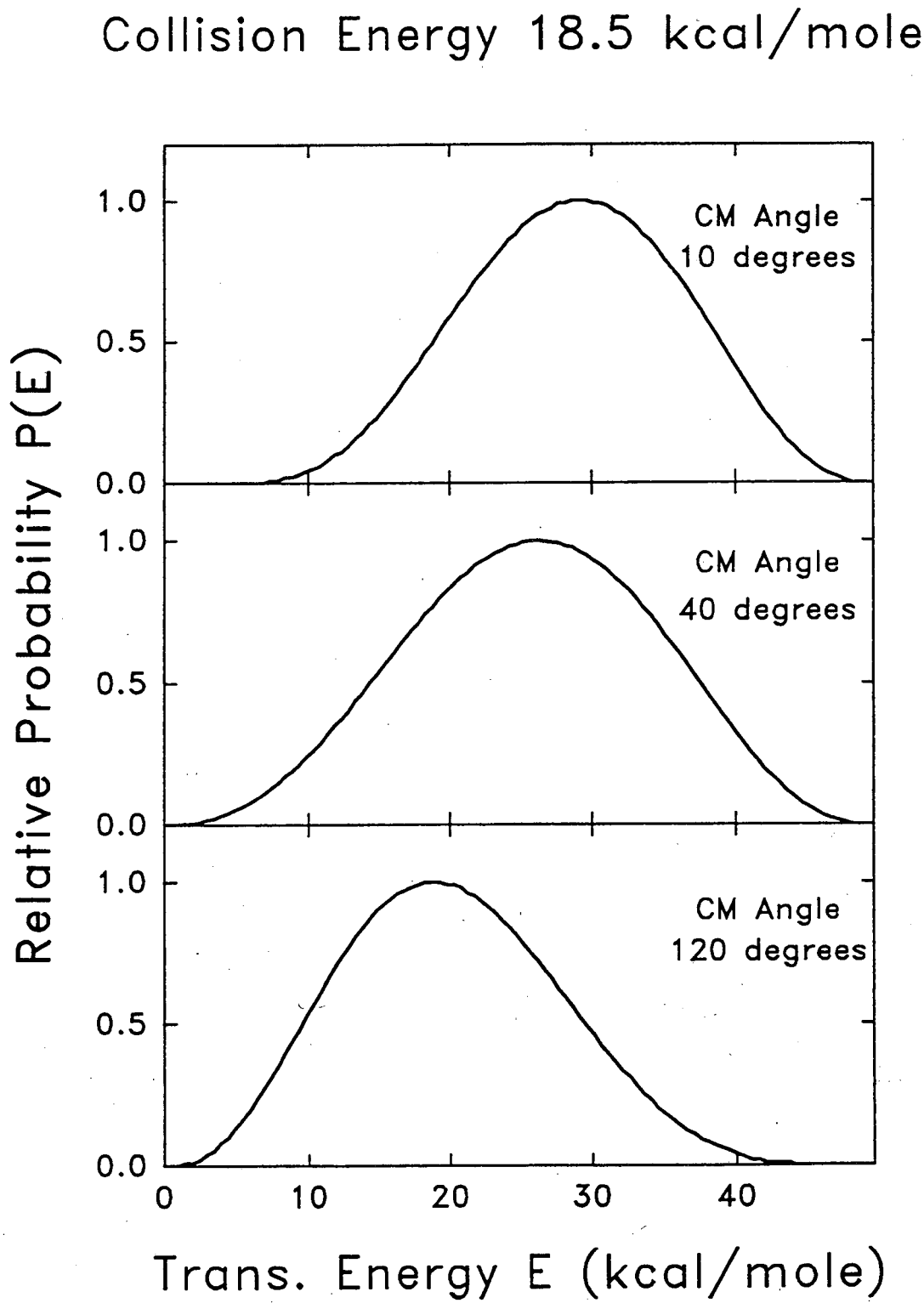
Collision Energy 18.5 kcal/mole
Relative Probability P(E)
1.0
0.5
0.0
CM Angle
10 degrees
CM Angle
40 degrees
CM Angle
120 degrees
0
10
20
30
40
Trans. Energy E (kcal/mole)

10
Fig.

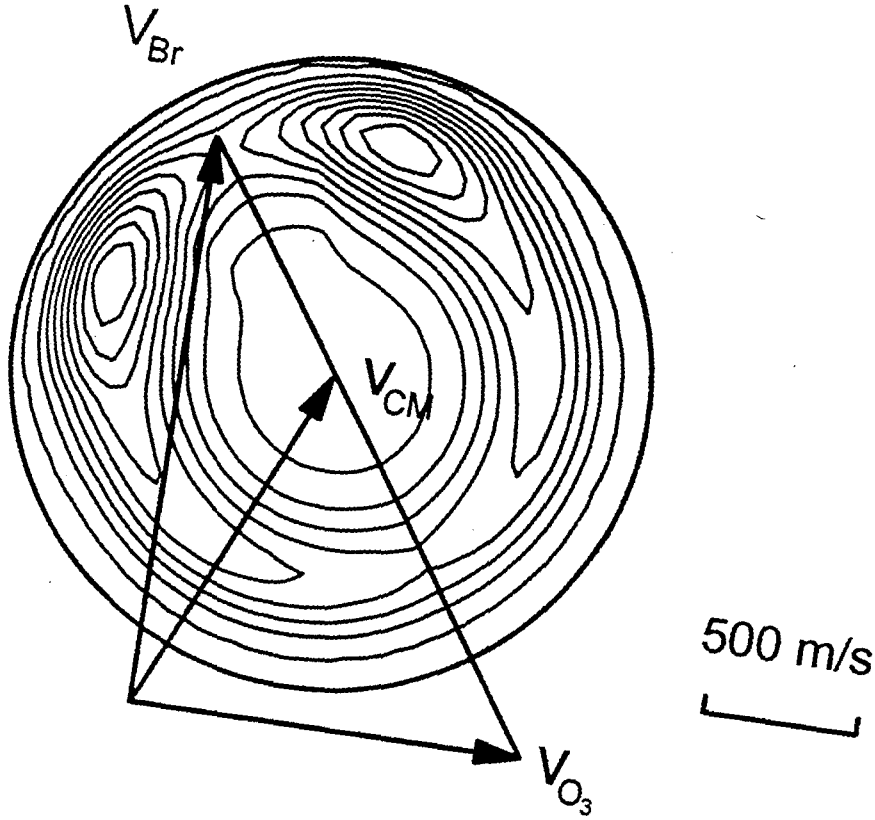
V_{Br}
V_{CM}
V_{O_3}
500 m/s

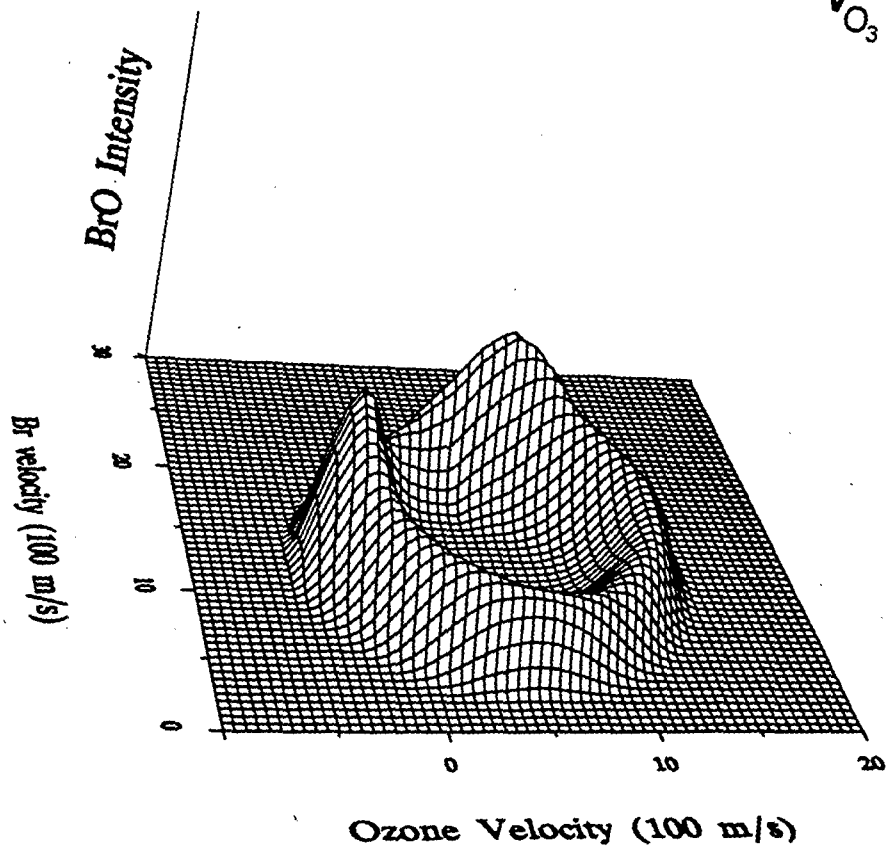
BrO Intensity
Br velocity (100 m/s)
0
10
20
30
0
10
20
Ozone Velocity (100 m/s)

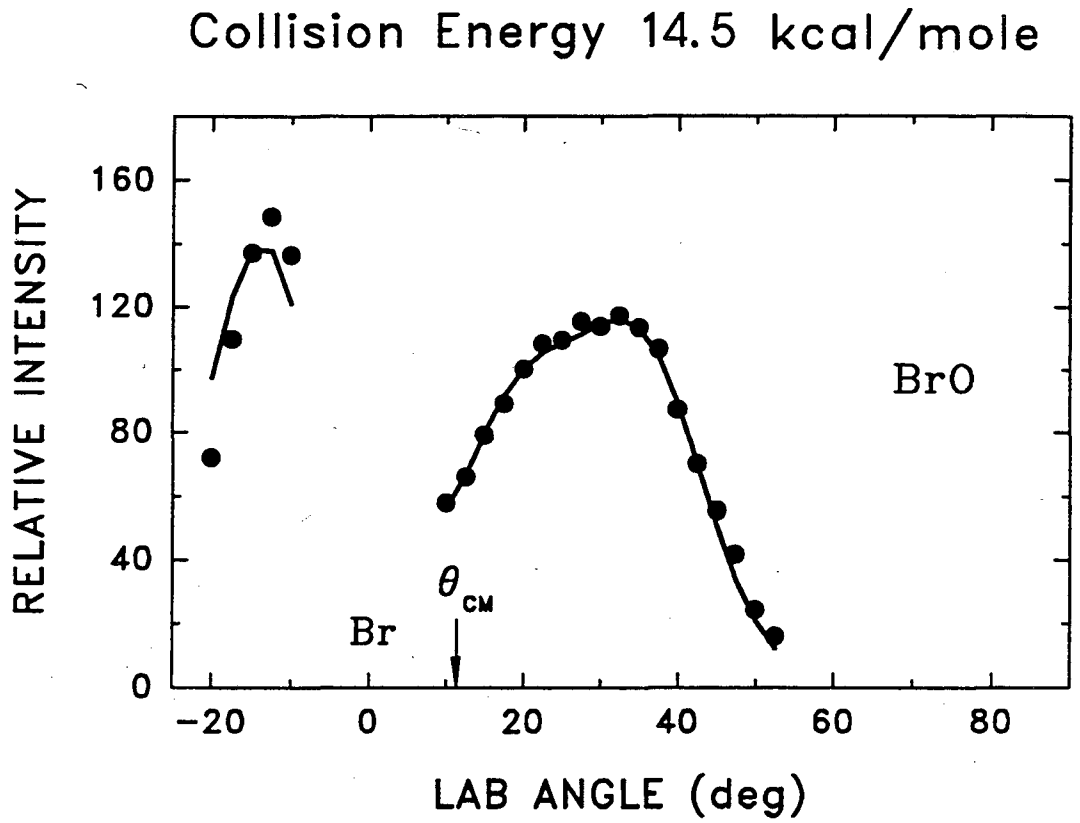
Collision Energy 14.5 kcal/mole
RELATIVE INTENSITY
160
120
80
40
0
−20
0
20
40
60
80
LAB ANGLE (deg)
Br
θ CM
BrO

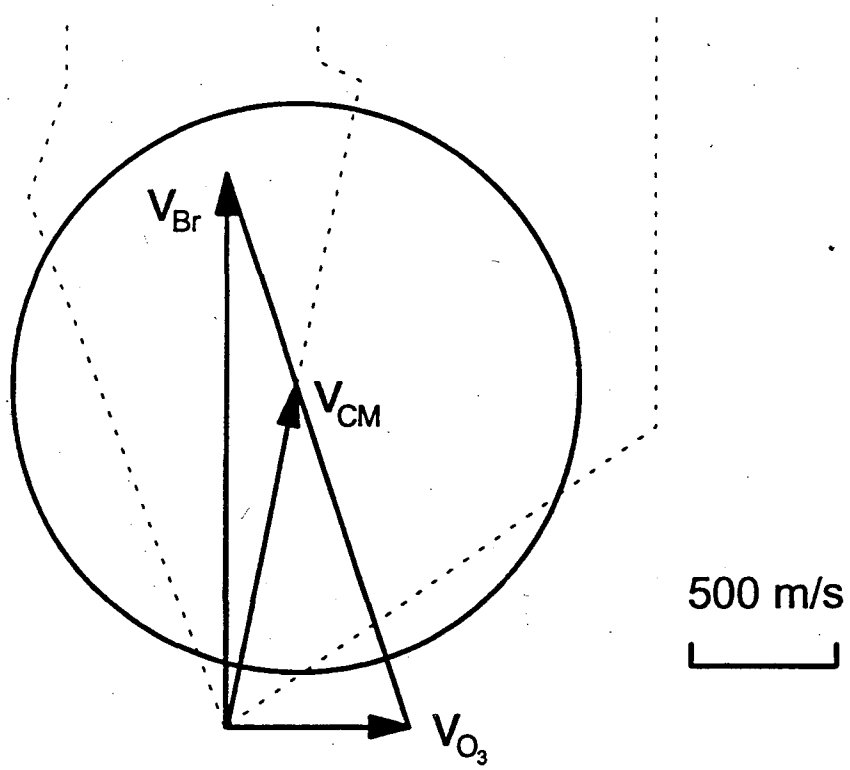
V Br
V CM
V O3
500 m/s

12

Fig.

$Br + O_3 \rightarrow BrO + O_2$ E_{coll} = 14.5 kcal/mole

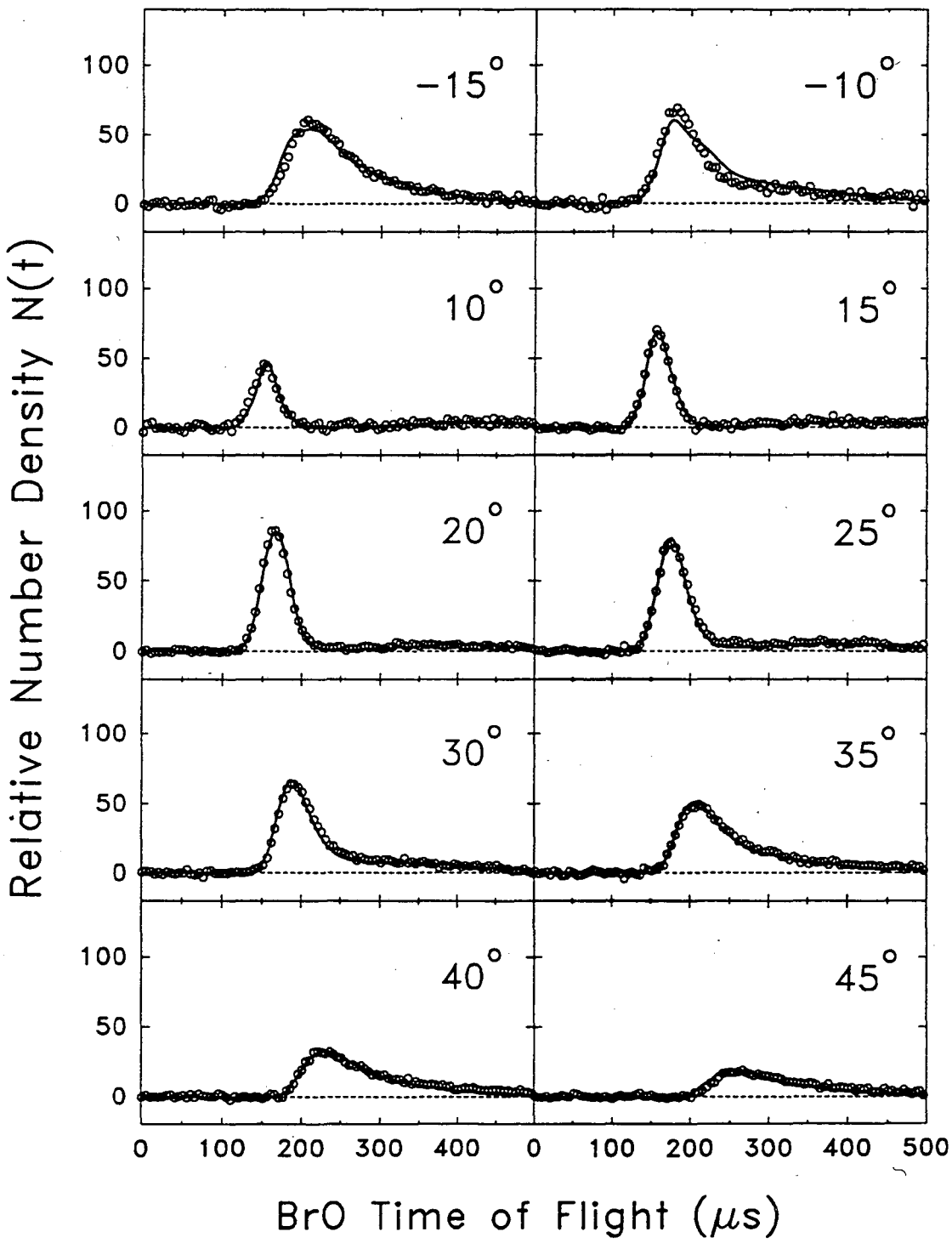

Fig. 5

Collision Energy 14.5 kcal/mole

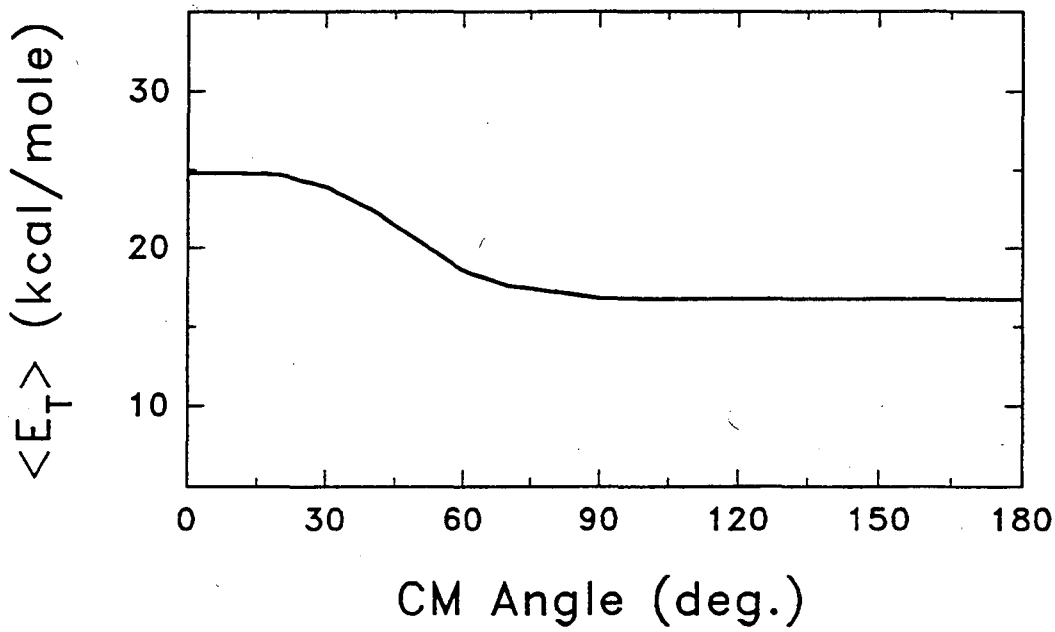

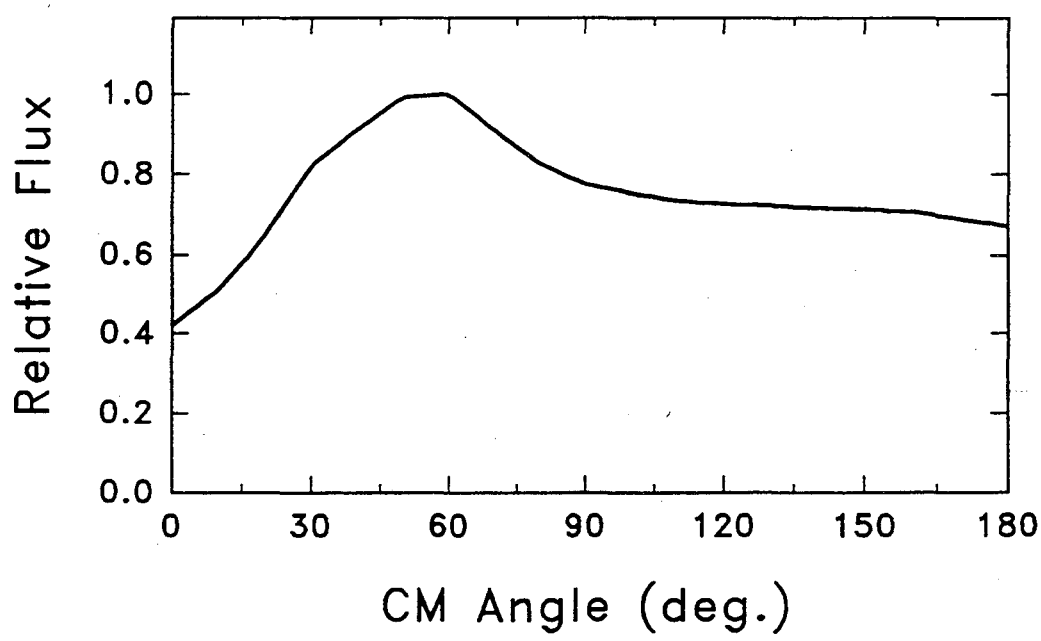

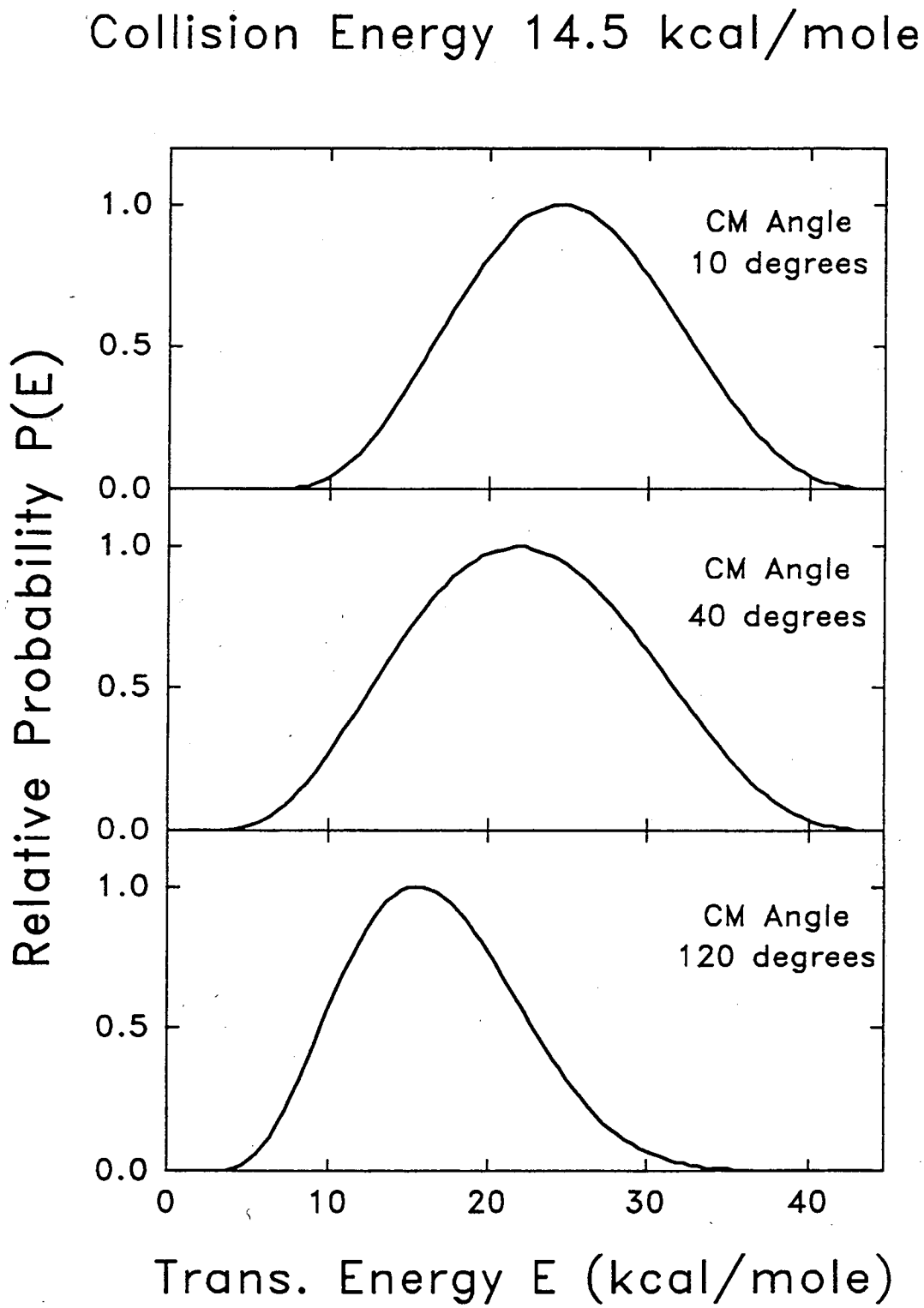
Collision Energy 14.5 kcal/mole
Relative Probability P(E)
1.0
0.5
0.0
CM Angle
10 degrees
CM Angle
40 degrees
CM Angle
120 degrees
0
10
20
30
40
Trans. Energy E (kcal/mole)

15

Fig. 1

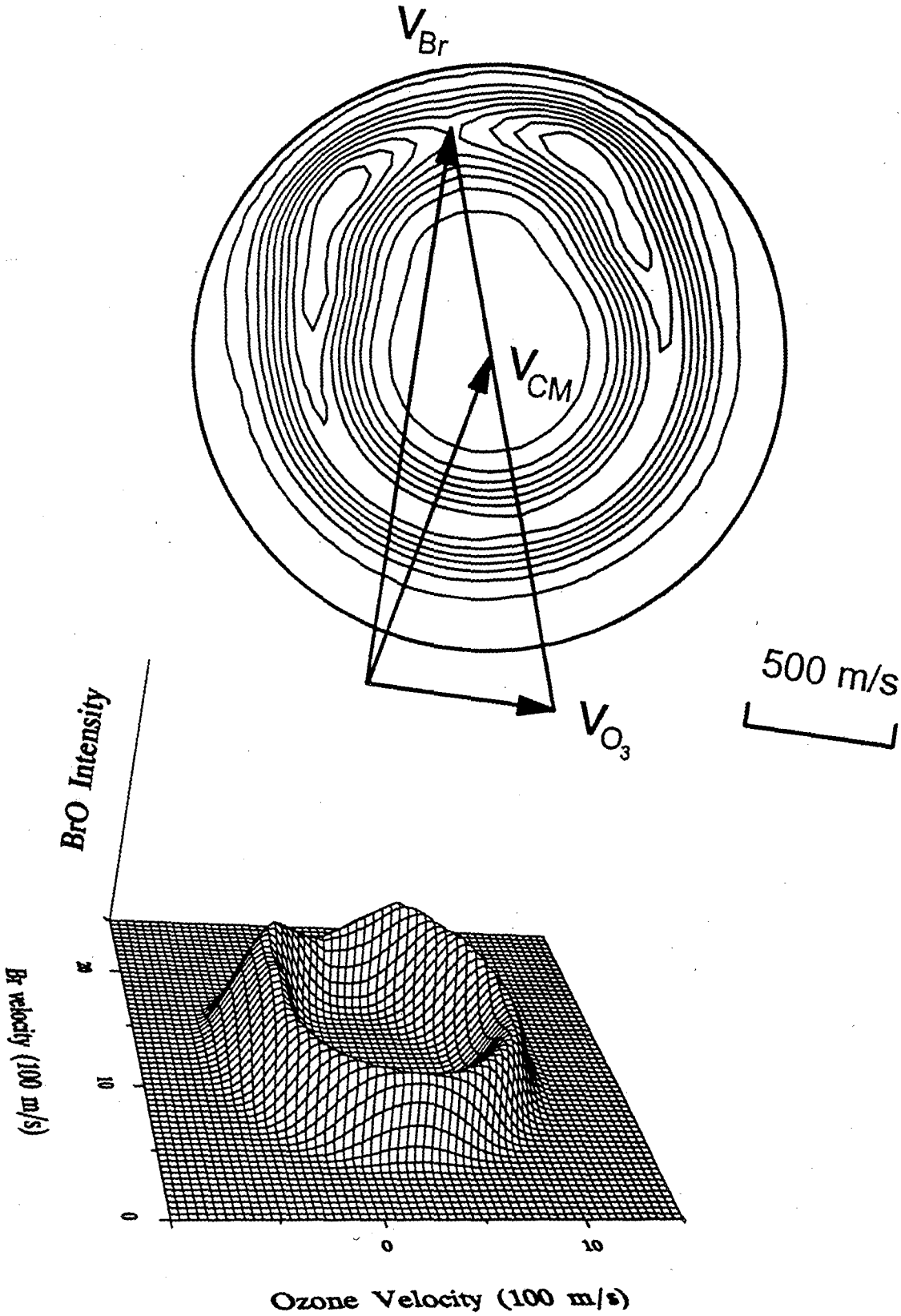
V_{Br}
V_{CM}
V_{O_3}
500 m/s
BrO Intensity
Br velocity (100 m/s)
0
10
20
0
10
Ozone Velocity (100 m/s)

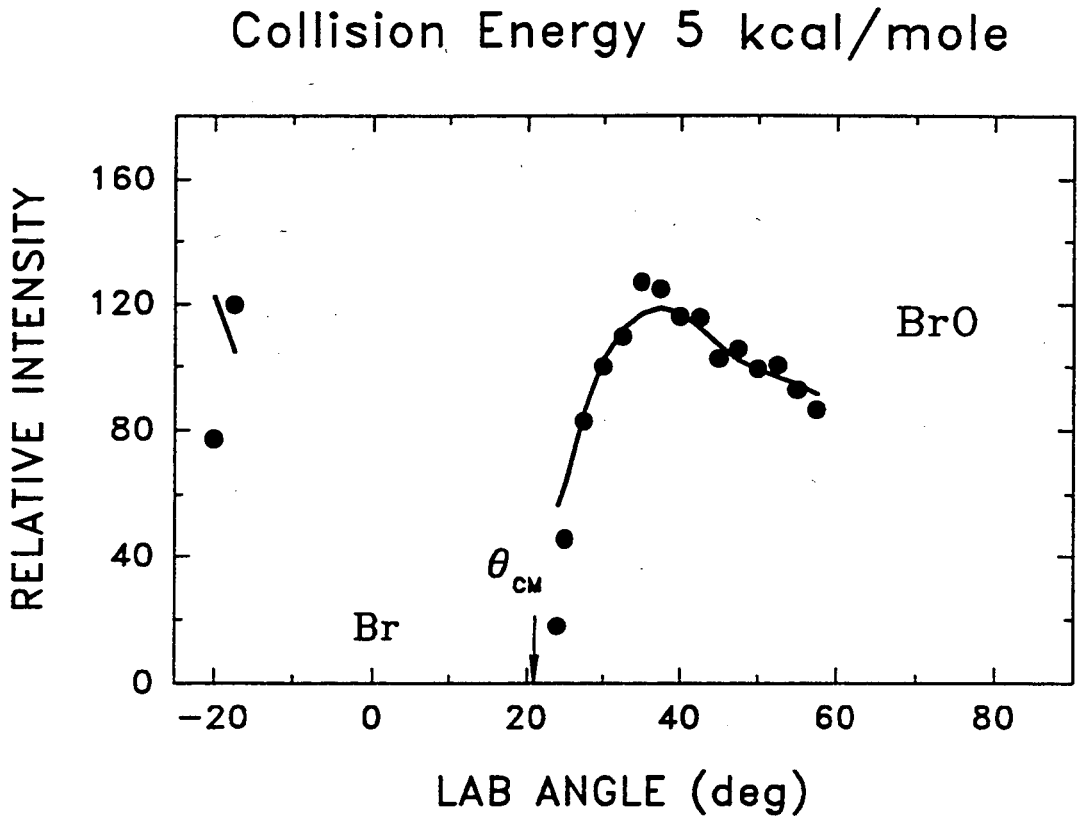
Collision Energy 5 kcal/mole
RELATIVE INTENSITY
160
120
80
40
0
−20
0
20
40
60
80
LAB ANGLE (deg)
BrO
Br
θ_{CM}

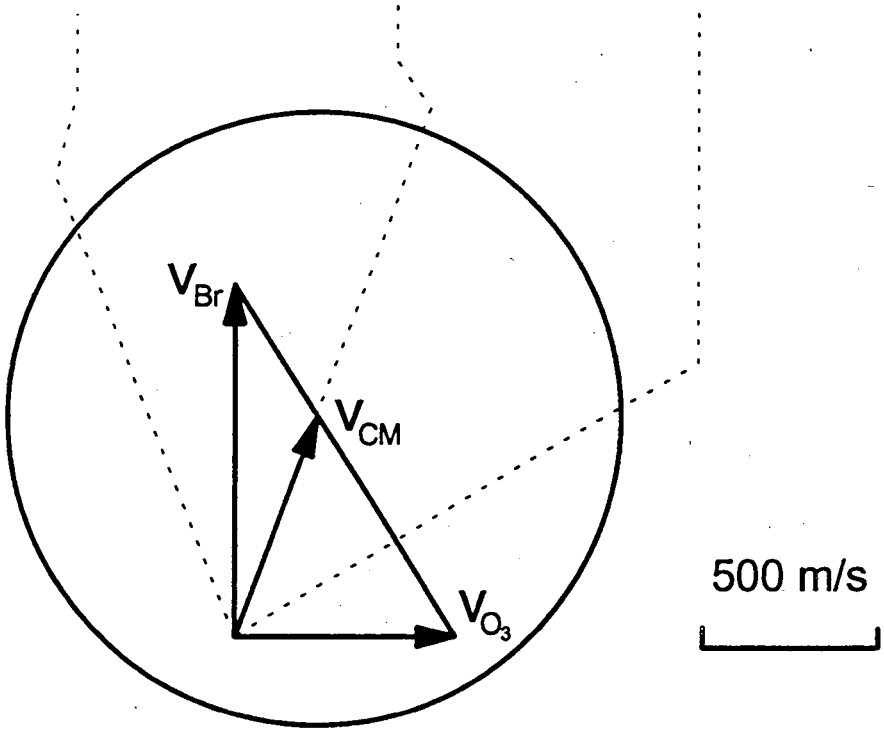
V_{Br}
V_{CM}
V_{O_3}
500 m/s

17

Fig.

$Br + O_3 \rightarrow BrO + O_2 \quad E_{coll} = 5$ kcal/mole

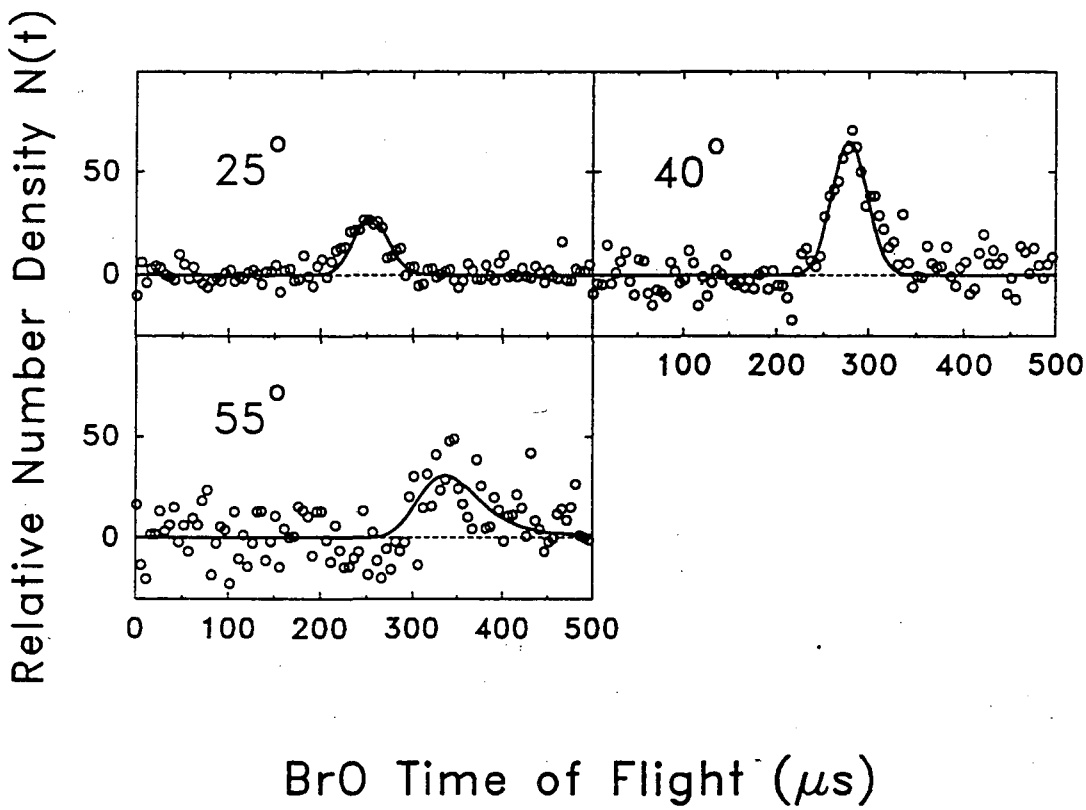

Fig. 1

Collision Energy 5 kcal/mole

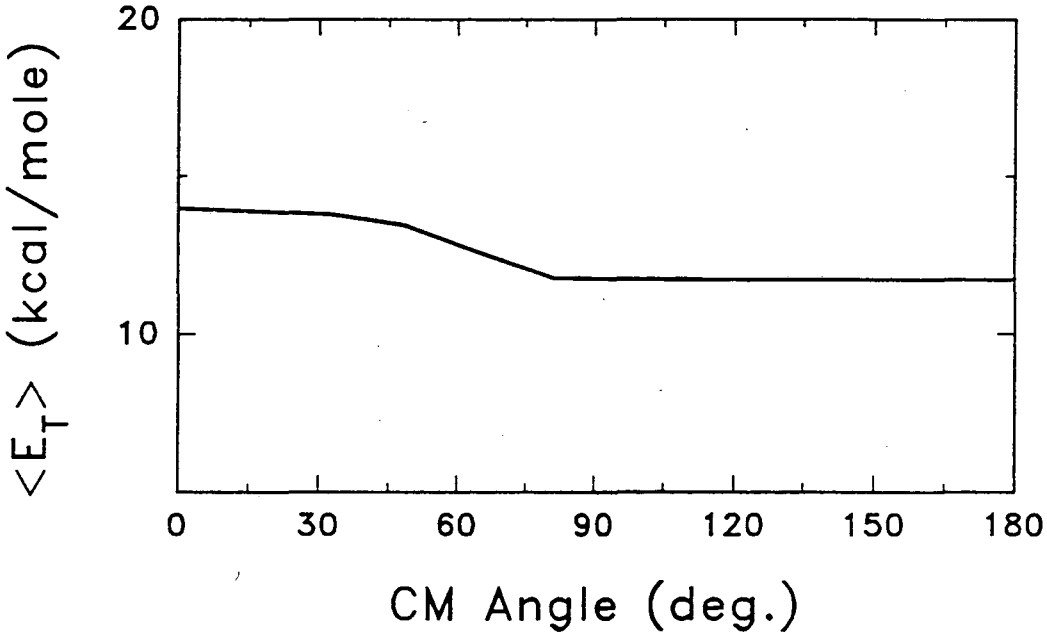

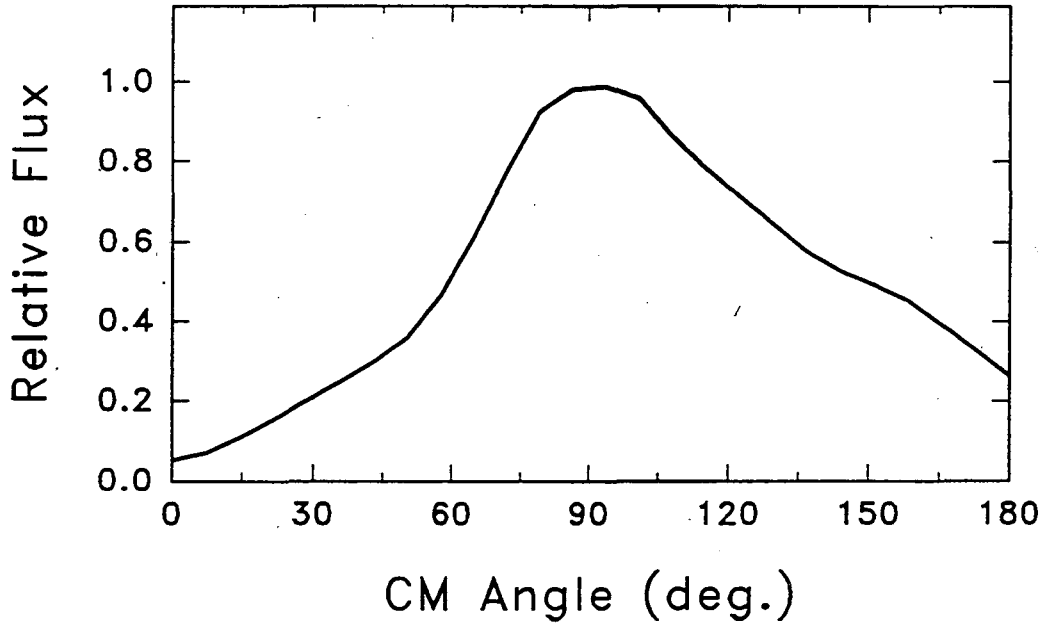

Fig. 1

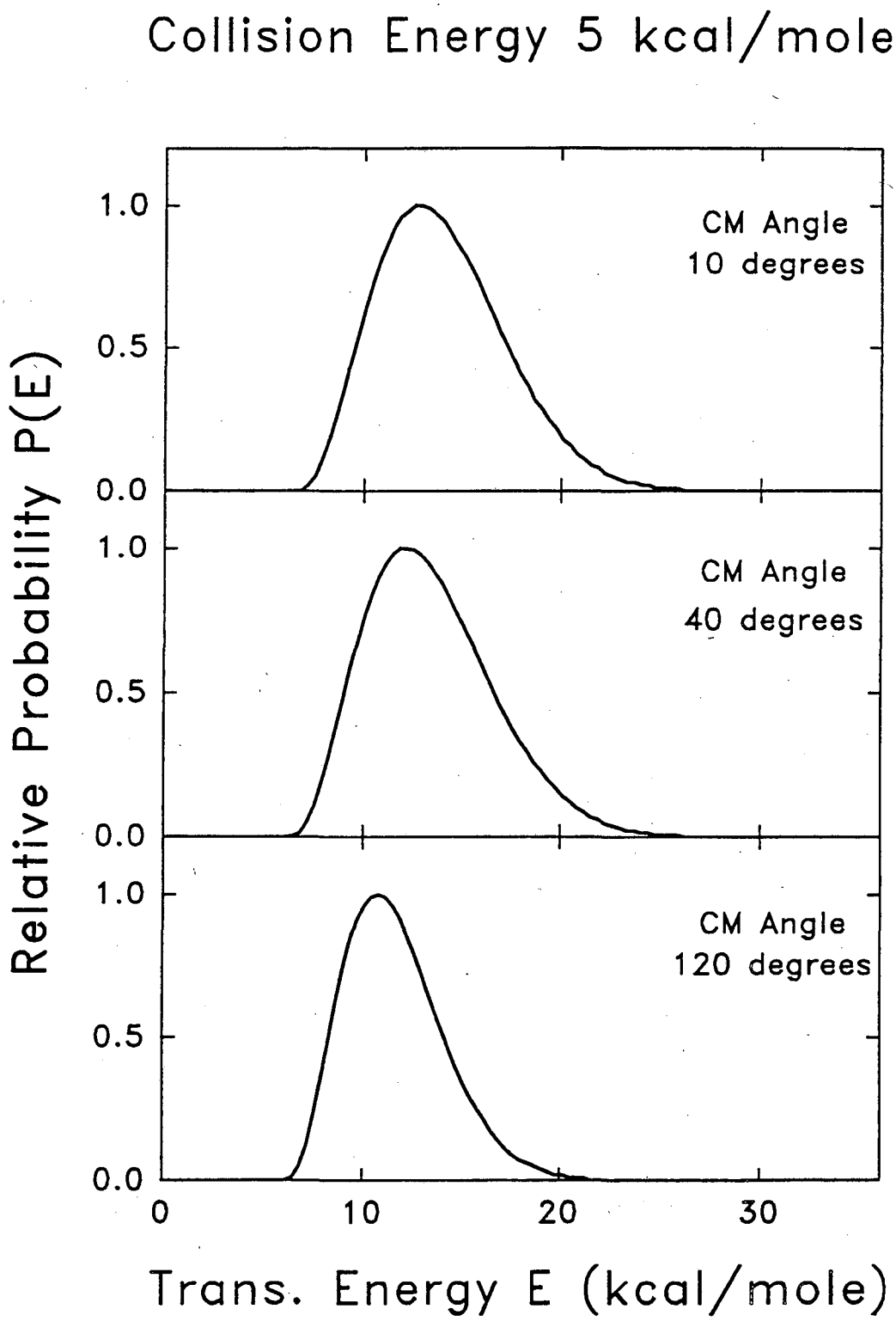
Collision Energy 5 kcal/mole
Relative Probability P(E)
1.0
0.5
0.0
CM Angle
10 degrees
CM Angle
40 degrees
CM Angle
120 degrees
0
10
20
30
Trans. Energy E (kcal/mole)

Fig.2

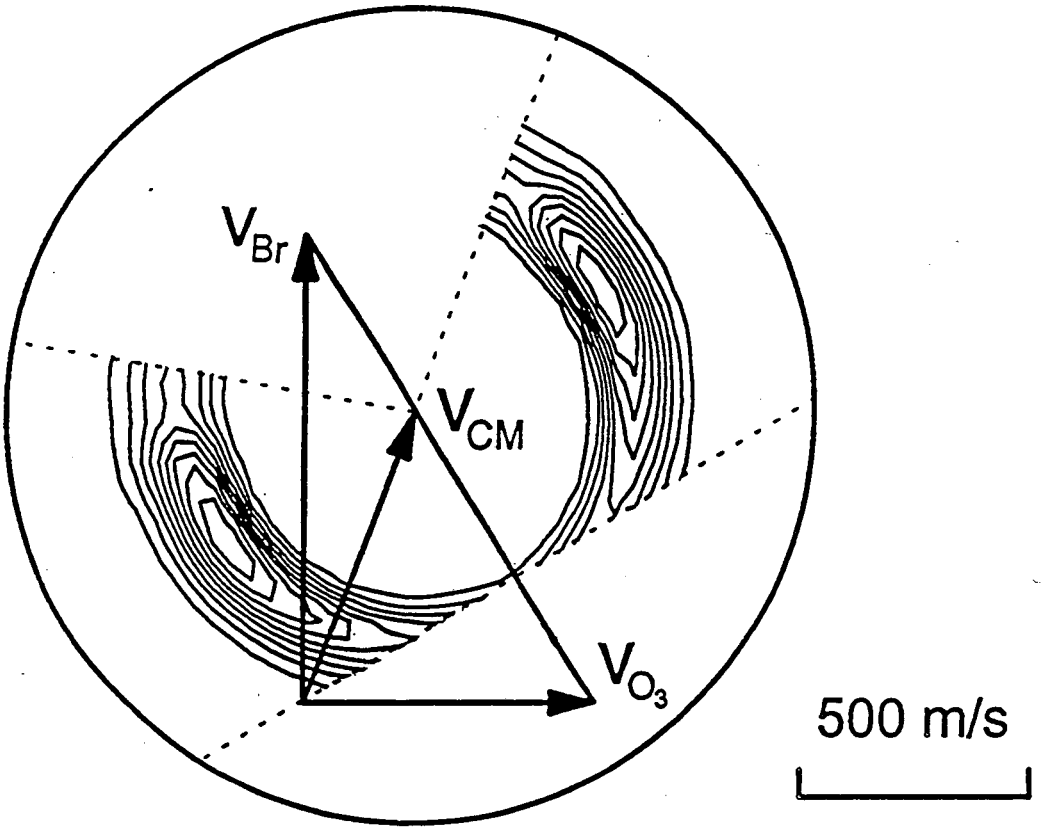

Fig.

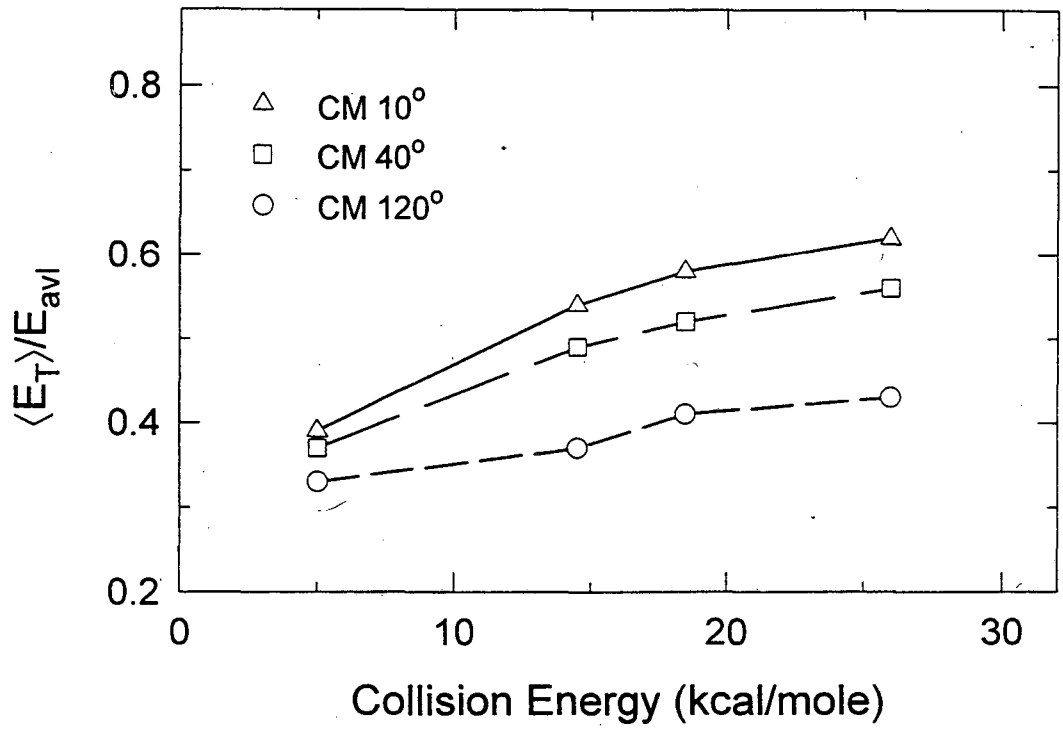
0.8
0.6
0.4
0.2
0
10
20
30
CM 10°
CM 40°
CM 120°
⟨E_T⟩/E_avl
Collision Energy (kcal/mole)

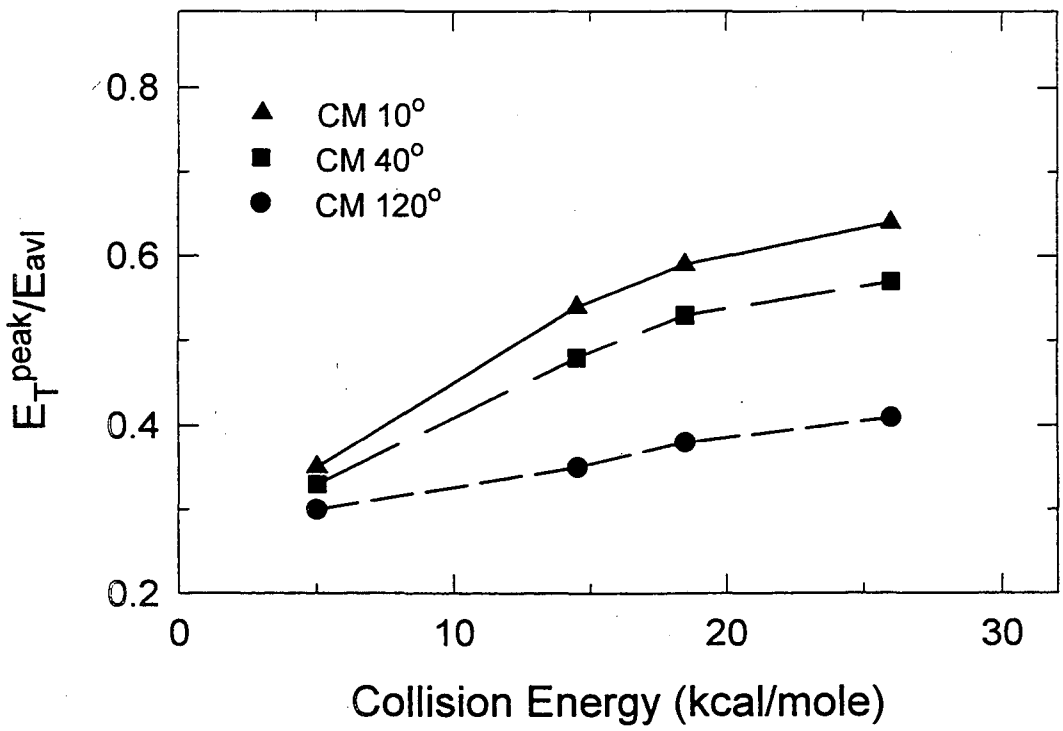
0.8
0.6
0.4
0.2
0
10
20
30
CM 10°
CM 40°
CM 120°
E_T^peak/E_avl
Collision Energy (kcal/mole)

Fig.:

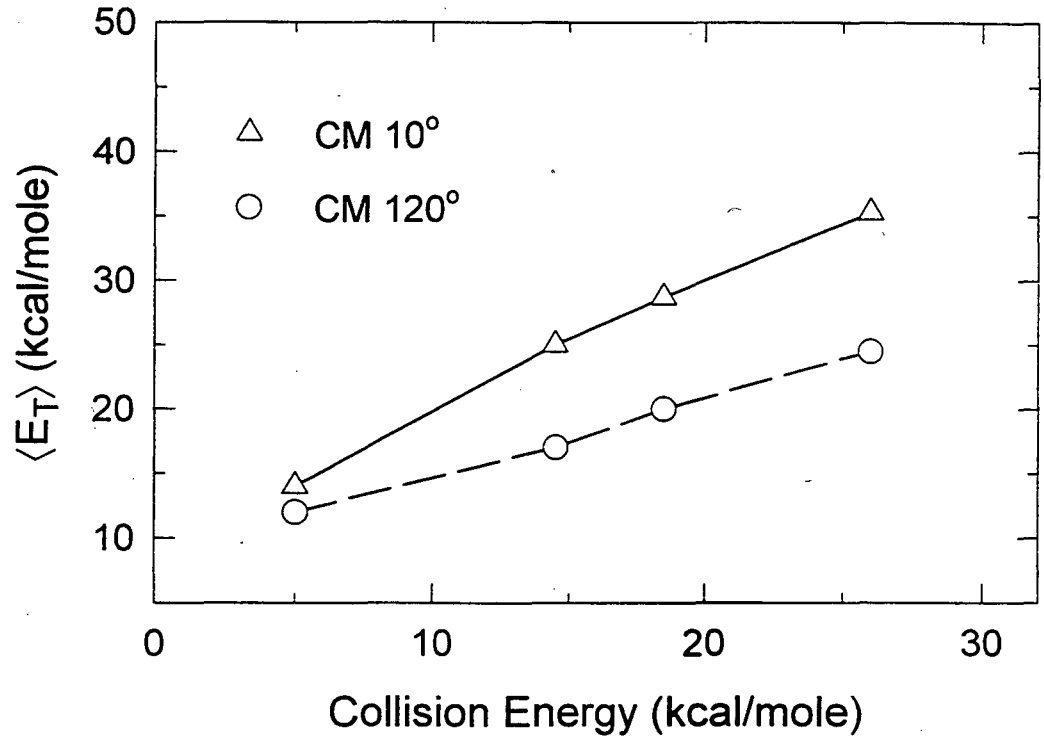
50
40
30
20
10
0
10
20
30
CM 10°
CM 120°
⟨E_T⟩ (kcal/mole)
Collision Energy (kcal/mole)

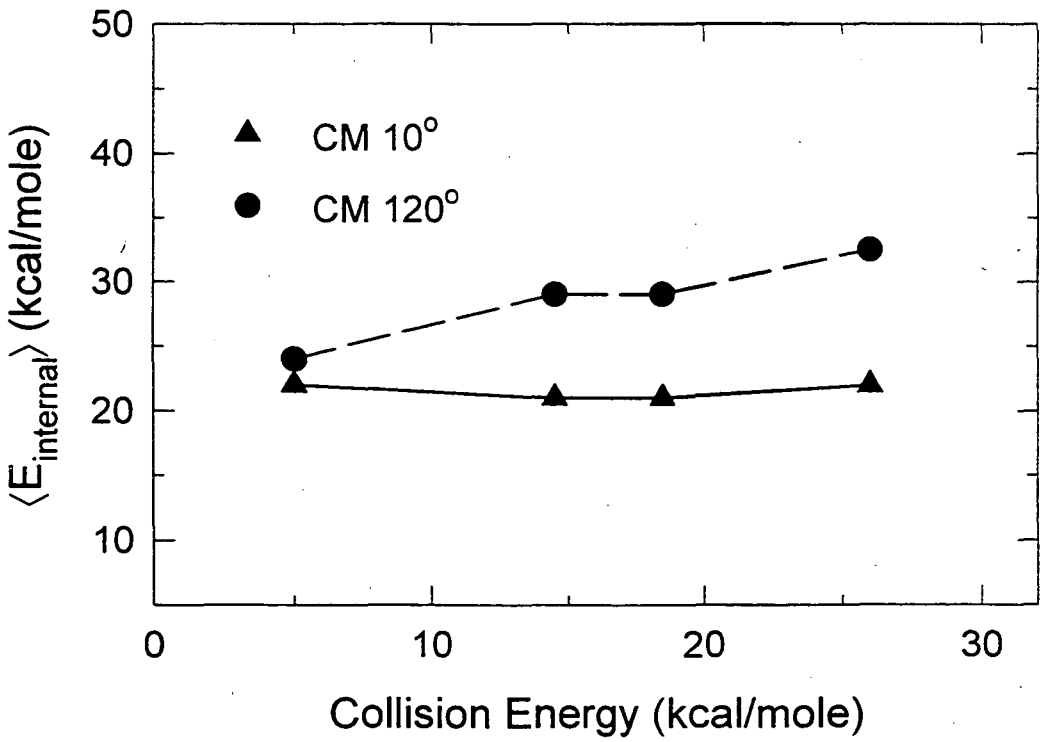
50
40
30
20
10
0
10
20
30
CM 10°
CM 120°
⟨E_internal⟩ (kcal/mole)
Collision Energy (kcal/mole)

23
Fig.

ERNEST ORLANDO LAWRENCE BERKELEY NATIONAL LABORATORY
ONE CYCLOTRON ROAD | BERKELEY, CALIFORNIA 94720

Prepared for the U.S. Department of Energy under Contract No. DE-AC03-76SF00098

AAE791
LBL Libraries